CAPITAL UNIVERSITY OF SCIENCE AND TECHNOLOGY, ISLAMABAD

MHD Thermal Boundary Layer Flow of Casson Fluid over a Penetrable Stretching Porous Wedge

by

Rimsha Shehzad

A thesis submitted in partial fulfillment for the degree of Master of Philosophy

in the

Faculty of Computing
Department of Mathematics

2023

Dedicated to my cherished parents, siblings, and respectable teachers who have taught me to work hard for the goals I have for myself.

CERTIFICATE OF APPROVAL

MHD Thermal Boundary Layer Flow of Casson Fluid over a Penetrable Stretching Porous Wedge

by

Rimsha Shehzad

(MMT203021)

THESIS EXAMINING COMMITTEE

S. No.	Examiner	Name	Organization
(a)	External Examiner	Dr. Nabeela Kousar	AIR University, Islamabad
(b)	Internal Examiner	Dr. M. Sabeel Khan	CUST, Islamabad
(c)	Supervisor	Dr. Dur-e-Shehwar Sagheer	CUST, Islamabad

Dr. Dur-e-Shehwar Sagheer
Thesis Supervisor
May, 2023

Dr. Muhammad Sagheer
Head
Dept. of Mathematics
May, 2023

Dr. M. Abdul Qadir
Dean
Faculty of Computing
May, 2023

Author's Declaration

I, **Rimsha Shehzad** hereby state that my MPhil thesis titled "**MHD Thermal Boundary Layer Flow of Casson Fluid over a Penetrable Stretching Porous Wedge**" is my own work and has not been submitted previously by me for taking any degree from Capital University of Science and Technology, Islamabad or anywhere else in the country/abroad.

At any time if my statement is found to be incorrect even after my graduation, the University has the right to withdraw my Mphil Degree.

(Rimsha Shehzad)

Registration No: MMT203021

Plagiarism Undertaking

I solemnly declare that research work presented in this thesis titled "**MHD Thermal Boundary Layer Flow of Casson Fluid over a Penetrable Stretching Porous Wedge**" is solely my research work with no significant contribution from any other person. Small contribution/help wherever taken has been duly acknowledged and that complete thesis has been written by me.

I understand the zero tolerance policy of the HEC and Capital University of Science and Technology towards plagiarism. Therefore, I as an author of the above titled thesis declare that no portion of my thesis has been plagiarized and any material used as reference is properly referred/cited.

I undertake that if I am found guilty of any formal plagiarism in the above titled thesis even after award of MPhil Degree, the University reserves the right to withdraw/revoke my MPhil degree and that HEC and the University have the right to publish my name on the HEC/University website on which names of students are placed who submitted plagiarized work.

(Rimsha Shehzad)

Registration No: MMT203021

Acknowledgement

First of all, I would like to thank **Almighty Allah** who is the most merciful and most beneficent to his creation. I also express my gratitude to the last messenger of **Almighty Allah**, **Prophet Muhammad (PBUH)** and the greatest propagator of knowledge for people.

I am thankful for the precious blessing from **Almighty Allah**, my parents and my siblings for their love and support. My father **Atif Qayyum** the diligent and my mother **Qurat-ul-ain** the forbearing they always have a trust in me that I will be at the hurdles and proceed with my life.

I am especially grateful to my respected supervisor **Dr. Dur-e-Shehwar Sagheer**. She not only guide me in my thesis but also in my personality guidance. I want to thank her from the bottom of my heart for always being available for discussion of this thesis despite her incredibly hectic schedule.

I would like to pay great tribute to all my professors **Dr. Muhammad Sagheer, Dr. Rashid Ali, Dr. Abdul Rehman Kashif** and **Dr. Samina Rashid**.

I would like to express a special gratitude to my mentor and inspiration **Dr. Shafqat Hussain**, the one who gives me every aspect of guideline whenever I call him for help.

Last but not the least my bestest friend **Mutayba Rafique**. Thanks for your support in every phase of my life. She is the person who encourages me that I can do my best in every exam of life.

(Rimsha Shehzad)

Registration No: MMT203021

Abstract

This thesis proposed the mathematical modeling of magneto hydro dynamics MHD thermal boundary layer flow using Casson fluid over an extending wedge by considering porosity, ohmic heating, viscous dissipation and convective boundary layer conditions. MHD fluid flow in different geometries is an interesting topic due to its application in medical science, radiation therapy, MHD generators, soil machincs, melt spinning process and insullations. The model of the problem consists a system of partial differential equation which is firstly non-dimensionalized to obtain non-linear ordinary differential equations. The obtained BVP is solved by using shooting technique which is endowed with Runge-Kutta method of order four and Newton method. The impact of different parameters on momentum and temperature fields is investigated. Tables and graphs are provided to examine the computational outcomes of surface drag force and Nusselt number. The significant observation are that by increasing the value of Casson parameter δ with velocity ratio parameter $R = 0.1$, the velocity profile increases and at $R = 2$, velocity profile decreases. Furthermore, by the rising value of Casson parameter δ at the velocity ratio parameter $R = 0.5$, the temperature profile increases and at $R = 2.1$, temperature profile decreases. Numerical tables are used to describe computational results for temperature, heat transfer rate, drag force, and velocity. It is highlighted that the rate of heat transmission was accelerated by the convective parameter.

Contents

List of Figures

List of Tables

Abbreviations

BCs	Boundary Conditions
BL	Boundary Layer
BVP	Boundary Value Problem
CF	Casson Fluid
CNG	Compressed Natural Gas
DTM	Differential Transformation Method
HAM	Homotopy Analysis Method
IVP	Initial Value Problem
MHD	Magneto Hydro Dynamics
ODEs	Ordinary Differential Equations
PDEs	Partial Differential Equations
RK	Runge Kutta
VD	Viscous Dissipation

Symbols

(u, v)	Velocity Component
(x, y)	Cartesian Coordiante
B	Uniform Magnetic Field
T_∞	Ambient Temperature
T_f	Temperature of Stretching Wedge
U_w	Stretching Velocity of Wedge
U	Velocity far away from Wedge
v_w	Suction and Injection Velocity of Wedge
g	Gravity Field
Ω	Total Angle of the Wedge
q_r	Radiative Heat Flux
M	Magnetic Parameter
λ	Mixed Convective Parameter
Gr_x	Local Grashof Number
Re_x	Local Reynold Number
R	Velocity Ratio Parameter
C	Suction Parameter
Nr	Radiation Heat Transfer Parameter
Ec	Eckert Number
Pr	Prandtl Number
C_f	Skin Fricktion
Nu_x	Nusselt Number
δ	Casson Parameter

Bi	Biot Number
$(Da)^{-1}$	Darcy Inverse Parameter
α	Thermal Conductivity
ν	Kinematic Viscosity
β_0	Coefficient of Thermal Expansion
σ	Conductivity of Fluid due to Electric Current
ρ	Fluid Density
c_p	Heat Capacity
α_1	Local Inertia Parameter
	Stream Function
β	Wedge Angle Parameter

Chapter 1

Introduction

The field of physics known as fluid mechanics studies how fluids behave both at rest and in motion. It has applications in many disciplines, for instance mechanical, aeronautical, civil, chemical and biomedical engineering, as well as geophysics, oceanography, meteorology, astrophysics, and biology.

The process convection involves the movement of heat from one point to the other point due to the bulk motion of a fluid. Convective heat transfer is the combination of two processes conduction and advection. Mixed convection across an impermeable or permeable wedge is used in many manufacturing processes, including the extrusion of molten polymers, the fabrication of plastic sheets for solar energy, and the storage of thermal energy. Karwe and Jaluria [1, 2] explained that this investigation is necessary to check the quality of resulting products and cooling rates. Ishak et al. [3] investigated the flow of magneto hydro dynamic mixed convection BL across a vertical sheet that was stretching while the wall temperature remains unchanged. The results of the ohmically dissipated slip flow of magneto hydro dynamic fluid across a radiating magnified surface were discussed by Bilal et al. [4].

The time-dependent problem of mixed convective flow over a vertical wedge was examined by Ravindran et al. [5]. Kumari and Nath [6] have investigated the unsteady MHD flow over an impulsively magnified absorptive vertical surface in a quiescent fluid. By Ganapathirao and Ravindran [7],investigations have been done into the problem of the vertical wedge with chemical reaction into mixed convective MHD flow in the presence of non-uniform slot suction/injection. Authors used an implicit finite difference approach together with a quasi-linearization scheme to produce findings that were dissimilar. Ullah et al. [8] emphasised the heat transfer features of MHD Falkner-Skan Casson fluid along with a moving wedge, where finite difference technique along with a quasi linearization method used to derive the solutions of nonlinear coupled PDEs after nondimensionalizing the governing equations and BCs by a nonsimilar transformations. They discovered that, in the existence of accelerating or decelerating flow, suction or injection significantly changes the rates of skin friction, concentration, and heat transfer. The unsteady mixed convective flow of a dusty fluid across a vertical wedge was studied by Hossain et al. [9].

A lot of above described studies addressed the convection flow over a vertical wedge. It is worth to mention that there are limited number of research about convetion flow in the presence of suction/injection, ohmic and viscous dissipation over a permeable/impermeable wedge. The approximate solution of the thermal radiation influence on MHD forced convection flow adjacent to nonisothermal fixed wedge with heat source/sink was computed by Chamkha et al. [10] using the implicit finite difference technique. Hossain et al. [11] have studied the problem of MHD flow via a wedge with changeable surface temperature. Su et al. [12] investigated the MHD mixed convective flow of heat transfer across a permeable stretched wedge using numerical and DTM methods. Also, authors demonstrated that as a domain becomes unbounded, the DTM solutions diverge.

The effects of chemical reaction on the MHD mixed convective flow of heat and mass transfer across a porous wedge were investigated by Kandasamy et al. [13]. Without taking the effects of magnetic fields, Hayat et al. [14] investigated the flow of a power-law fluid past a wedge while maintaining the wedge's fixed surface. The issue of MHD flow through a porous non-isothermal wedge was examined by Prasad et al. [15]. The impacts of VD, joule heating, and stress work was also discussed and arrived at the numerical solutions using finite difference method.

The issue of a non-isothermal wedge and non-newtonian Jeffrey's fluid was covered by Gaffar et al. [16]. They used the implicit keller box approach for finite differences. Unsteady Falkner-Skan flow of carreau nanofluid via a static/moving wedge was studied by Khan et al. [17].

Due to the numerous applications in radiation therapy, ceramic engineering, metal casting technology, etc., numerous studies have been managed to explore the effects of radiation on BL flow with transfer of heat characteristics. Ganesh et al. [18] have studied the issue of magneto-marangoni nanofluid boundary layer flow in the presence of non-linear thermal radiation. A different approach was made by Ganesh et al. [19], who investigated the flow of gamma AL_2O_3 nanofluids over a stretched sheet using non-linear thermal radiation. Ullah et al. [20] have investigated the casson fluid flow across a moving wedge using thermophoresis and a brownian diffusion mechanism. The heat transport phenomena with homogeneous-heterogeneous CF flow in a porous media were studied by lal et al. [21]. A number of researchers investigated the impact of heat radiation on different flow problems [22–24]. The results of non-Fourier double diffusions theories to the CF across an elongating sheet were more recently examined by Sohail et al. [25]. For numerical solutions authors used the optimum homotopy analysis approach. Another effort was made by Sohail et al. [26], for the investigation of MHD casson model entropy production, where the thermal conductivity and fluctuating heat was also considered.

1.1 Thesis Contributions

In this thesis, the work of Hussain et al.[27] is discussed in detail. The problem of non-Newtonian flow of Casson fluid over a stretching wedge with ohmic heating and convective boundary layer condition is examined. Hussain et al.[27] used homotopy analysis method (HAM) for the numerical solutions. We utilized shooting technique for numerical solutions to analyse the influence of various emerging parameters on velocity and temperature profiles. The findings of the problem can be a notable addition in literature. Furthermore, we extended the problem of Hussain et al.[27] by considering the porous medium and viscous dissipation. The flow model is a system of partial differential equations. These equations are converted into a system of ordinary differential equations using suitable transformations. Approximate solutions for this boundary value problem are obtained by using the shooting method. At the end of this thesis, the effect of physical parameters over velocity $f'(\eta)$ and temperature $\theta(\eta)$ profiles are described through tables and also by graphs. Computational outcomes of surface darg force and Nusselt number are also displayed through tables and graphs. MATLAB inbuilt command bvp4c is also applied to validate the code and authenticate the accuracy of findings.

1.2 Layout of Thesis

The following is a brief summary of the thesis's content.

Chapter 2

The chapter provides a list of fundamental definitions. These terminologies facilitate to uderstand the concepts discussed in subsequent chapters.

Chapter 3

This chapter provides the detailed review of the work done by Hussain et al.[27]. In [27] the governing set of PDEs is transformed into set of ODEs by applying appropriate similarity transformations. These equations are further solved by using shooting method.

Chapter 4

This chapter provides the extension of the problem discussed by Hussain et al.[27] by adding effects of porosity and viscous dissipation. The system of partial differential equations is converted into a set of ordinary differential equations by applying appropriate similarity transformations. These equations are further solved by using shooting method. Eventually the accquired numerical results are explained through the graphical results and tables.

Chapter 5 This chapter dispenses the conclusion of the thesis.

References cited in the thesis are included in the **bibliography**.

Chapter 2

Preliminaries

This chapter contains some basic definitions and governing laws, which will be helpful in the subsequent chapters.

2.1 Some Basic Terminologies

Definition 2.1.1 (Fluid)
"A substance exists in three primary phases solid, liquid, and gas. At very high temperatures, it also exists as plasma. A substance in the liquid or gas phase is referred to as a fluid." [29]

Definition 2.1.2 (Fluid Mechanics)
"Fluid mechanics is defined as the science that deals with the behavior of fluids at rest (fluid statics) or in motion (fluid dynamics)." [29]

Definition 2.1.3 (Density)
"Density or mass density of a fluid is defined as the ratio of the mass of a fluid to its volume. Mathematically,

$$\rho = \frac{mass\ of\ a\ fluid}{volume\ of\ a\ fluid},$$

The SI unit of density is kg per cubic meter (kg/m^3)." [29]

Definition 2.1.4 (Fluid Dynamics)

"The study of fluid if the pressure forces are also considered for the fluids in motion, that branch of science is called fluid dynamics." [30]

Definition 2.1.5 (Fluid Statics)

"The study of fluid at rest is called fluid statics." [30]

Definition 2.1.6 (Viscosity)

"Viscosity is defined as the property of a fluid which offers resistance to the movement of one layer of fluid over another adjacent layer of the fluid. Mathematically,

$$\mu = \frac{\tau}{\frac{du}{dy}},$$

where μ is viscosity coefficient, τ is shear stress and $\frac{\partial u}{\partial y}$ represents the velocity gradient. The SI unit of μ is $Pa.s.$ or Ns/m^2. " [30]

Definition 2.1.6 (Kinematic Viscosity)

"It is defined as the ratio between the dynamic viscosity and density of fluid. It is denoted by symbol ν called **'nu'**. Mathematically,

$$\nu = \frac{\mu}{\rho}$$

where μ denotes dynamic viscosity and ρ denotes density respectively. The unit of ν is m^2/sec." [30]

Definition 2.1.6 (Viscous Dissipation)

"The rate of work against internal stresses is slightly more complicated in compressible fluids" [31]

Definition 2.1.7 (Thermal Conductivity)

"The Fourier heat conduction law states that the heat flow is proportional to the temperature gradient. The coefficient of proportionality is a material parameter known as the thermal conductivity which may be a function of a number of variables. The SI unit of Thermal Conductivity is m^2/s." [29]

Definition 2.1.8 (Thermal Diffusivity)

"The rate at which heat diffuses by conducting through a material depends on the thermal diffusivity and can be defined as,

$$\alpha = \frac{k}{\rho C_p},$$

where α is the thermal diffusivity, k is the thermal conductivity, ρ is the density and C_p is the specifc heat at constant pressure. The SI unit of thermal diffusivity is m^2/s." [32]

2.2 Types of Fluid

Definition 2.2.1 (Ideal Fluid)

"A fluid, which is incompressible and has no viscosity, is known as an ideal fluid. Ideal fluid is only an imaginary fluid as all the fluids, which exist, have some viscosity." [30]

Definition 2.2.2 (Real Fluid)

"A fluid, which possesses viscosity, is known as a real fluid. In actual practice, all the fluids are real fluids." [30]

Examples of real fluids are water, juices and CNG etc.

Definition 2.2.3 (Newtonian Fluid)

"A real fluid, in which the shear stress is directly proportional to the rate of shear strain (or velocity gradient), is known as a Newtonian fluid." [30]
Example of Newtonian fluid is water.

Definition 2.2.4 (Non-Newtonian Fluid)

"A real fluid in which the shear stress is not directly proportional to the rate of shear strain (or velocity gradient), is known as a non-Newtonian fluid. [30]

$$\tau_{xy} \propto \left(\frac{du}{dy}\right)^m, \qquad m \neq 1$$
$$\tau_{xy} = \mu\left(\frac{du}{dy}\right)^m."$$

Examples of non-newtonian fluids are peri peri sauce, mustard sauce and lotions.

Definition 2.2.5 (Casson Fluid)

"Casson fluid can be defined as a shear thinning liquid which is assumed to have an infinite viscosity at zero rate of shear, a yield stress below which no flow occurs, and a zero viscosity at an infinite rate of shear." [33]
Examples of casson fluids are blood, melted chocolate and shakes.

Definition 2.2.6 (Magnetohydrodynamics)

"Magnetohydrodynamics(MHD) is concerned with the mutual interaction of fluid flow and magnetic fields. The fluids in question must be electrically conducting and non-magnetic, which limits us to liquid metals, hot ionised gases (plasmas) and strong electrolytes." [34]
Example is salt water.

2.3 Types of Fluid Flow

Different types of fluid flow are discussed in detail in this section:

Definition 2.3.1 (Rotational Flow)

"Rotational flow is that type of flow in which the fluid particles while flowing along stream-lines, also rotate about their own axis." [30]
Example is the air around the rotating fan blades of aeroplanes, ships and helicopters.

Definition 2.3.2 (Irrotational Flow)

"Irrotational flow is that type of flow in which the fluid particles while flowing along stream-lines, do not rotate about their own axis then this type of flow is called irrotational flow." [30]
Example is flow of river and water over a dam.

Definition 2.3.3 (Compressible Flow)

"Compressible flow is that type of flow in which the density of the fluid changes from point to point or in other words the density (ρ) is not constant for the fluid, Mathematically,

$$\rho \neq k,$$

where k is constant." [30]

Example is CNG.

Definition 2.3.4 (Incompressible Flow)

"Incompressible flow is that type of flow in which the density is constant for the fluid. Liquids are generally incompressible while gases are compressible, Mathematically,

$$\rho = k,$$

where k is constant." [30] Examples are water and petrol.

Definition 2.3.5 (Steady Flow)

"If the flow characteristics such as depth of flow, velocity of flow, rate of flow at any point in open channel flow do not change with respect to time, the flow is said to be steady flow. Mathematically,

$$\frac{\partial Q}{\partial t} = 0,$$

where Q is any fluid property." [30]

Definition 2.3.6 (Unsteady Flow)

"If at any point in open channel flow, the velocity of flow, depth of flow or rate of flow changes with respect to time, the flow is said to be unsteady. Mathematically,

$$\frac{\partial Q}{\partial t} \neq 0,$$

where Q is any fluid property." [30]

Definition 2.3.7 (Internal Flow)

"Flows completely bounded by a solid surfaces are called internal or duct flows." [29]

Definition 2.3.8 (External Flow)

"Flows over bodies immersed in an unbounded fluid are said to be an external flow." [29]

2.4 Modes of Heat Transfer

The three different types of heat transfer are described here.:

Definition 2.4.1 (Heat Transfer)

"Heat transfer is a branch of engineering that deals with the transfer of thermal energy from one point to another within a medium or from one medium to another due to the occurrence of a temperature difference." [35]

Definition 2.4.2 (Conduction)

"This is the mode of energy transfer as heat due to temperature difference within a body or between bodies in thermal contact without the involvement of mass flow and mixing." [32]

While considering a pan on a burning wood the transfer of heat from fire to pan is called conduction.

Definition 2.4.3 (Convection)

" This mode of heat transfer is met with in situations where energy is transferred as heat to a flowing fluid at the surface over which the flow occurs." [32]

Example is in boiling milk heat is being transfered from hotter to cooler area.

Definition 2.4.4 (Thermal Radiation)

"Thermal radiation is defined as radiant (electromagnetic) energy emitted by a medium and is due solely to the temperature of the medium." [35] Examples are X-rays and gamma rays.

2.5 Dimensionless Numbers

Following dimensionless numbers are crucial for the discussion of heat transfer in the fluid flow.

Definition 2.5.1 (Eckert Number)

"It is the dimensionless number used in continuum mechanics. It describes the relation between flows and the boundary layer enthalpy difference and it is used for characterized heat dissipation. Mathematically,

$$Ec = \frac{u^2}{C_p \nabla T},$$

where, u (ms^{-1}) is fluid flow velocity far from body, C_p denotes the specific heat capacity and ∇T is the temperature difference." [36]

Definition 2.5.2 (Prandtl Number)

"It is the ratio between the momentum diffusivity ν and thermal diffusivity α. Mathematically, it can be defined as

$$Pr = \frac{\nu}{\alpha} = \frac{\frac{\mu}{\rho}}{\frac{k}{C_p\rho}} = \frac{\mu C_p}{k},$$

where, μ represents the dynamic viscosity, Cp denotes the specific heat and k stands for thermal conductivity. The relative thickness of thermal and momentum boundary layer is controlled by Prandtl number. For small Pr, heat distributed rapidly corresponds to the momentum." [36]

Definition 2.5.3 (Skin Friction Coefficient)

"It expresses the dynamic friction resistance originating in viscous fluid flow around a fixed wall. The skin fricktion is defined by following mathematical formula:

$$C_f = \frac{2\tau_w}{\rho u_\infty^2},$$

where, τ_w denotes the wall shear stress, ρ is the fluid density and u_∞ free fluid flow." [36]

Definition 2.5.4 (Nusselt Number)

"It expresses the ratio of the total heat transfer in a system to the heat transfer by conduction. In characterizes the heat transfer by convection between a fluid and the environment close to it or, alternatively, the connection between the heat transfer intensity and the temperature field in a flow boundary layer. Mathematically,

$$Nu = \frac{qL}{k},$$

where q stands for the convection heat transfer, L for the characteristic length and k stands for thermal conductivity." [36]

Definition 2.5.6 (Reynolds Number)

"It is defined as the ratio of inertia force of a flowing fluid and the viscous force of the fluid. Mathematically,

$$Re = \frac{VL}{\nu},$$

where V denotes the free stream velocity, L is the characteristic length and ν stands for kinematic viscosity." [36]

2.6 Governing Laws

Numerous laws of conservation for example the law of conservation of mass, law of conservation of momentum and law of conservation of energy plays an important role while analysing a fluid flow problem. Firstly, these are applied on closed surfaces and then for analysis these surfaces are called control volumes.

Definition 2.6.1 (Conservation of Mass)

"The conservation of mass relation for a closed system undergoing a change is expressed as m_{sys} = constant or $\frac{dm_{sys}}{dt} = 0$, which is a statement of the obvious that the mass of the system remains constant during a process. For a control volume (CV), mass balance is expressed in the rate form as:

$$\dot{m}_{in} - \dot{m}_{out} = \frac{dm_{CV}}{dt},$$

where $\dot{m}_{in}$ and $\dot{m}_{out}$ are the total rates of mass flow into and out of the control volume, respectively, and $\frac{dm_{CV}}{dt}$ is the rate of change of mass within the control volume boundaries. In fluid mechanics, the conservation of mass relation written for a differential control volume is usually called the continuity equation." [29]

Definition 2.6.2 (Conservation of Momentum)

"The product of the mass and the velocity of a body is called the linear momentum or just the momentum of the body, and the momentum of a rigid body of mass m moving with a velocity $\vec{V}$ is $m\vec{V}$. Newton's second law states that the acceleration of a body is proportional to the net force acting on it and is inversely proportional to its mass, and that the rate of change of the momentum of a body is equal to the net force acting on the body. Therefore, the momentum of a system remains constant when the net force acting on it is zero, and thus the momentum of such systems is conserved. This is known as the conservation of momentum principle. In fluid mechanics, Newton's second law is usually referred to as the linear momentum equation, which is discussed in together with the angular momentum equation." [29]

Definition 2.6.3 (Conservation of Energy)

"Energy can be transferred to or from a closed system by heat or work, and the conservation of energy principle requires that the net energy transfer to or from a system during a process be equal to the change in the energy content of the system. Control volumes involve energy transfer via mass flow also, and the conservation of energy principle, also called the energy balance, is expressed as:

$$Conservation\ of\ energy: \quad \dot{E}_{in} - \dot{E}_{out} = \frac{dE_{CV}}{dt},$$

where, $\dot{E}_{in}$ and $\dot{E}_{out}$ are the total rates of energy transfer into and out of the control volume, respectively, and $\frac{dE_{CV}}{dt}$ is the rate of change of energy within the control volume boundaries. In fluid mechanics, we usually limit our consideration to mechanical forms of energy only." [29]

2.7 Shooting Method

Consider the following nonlinear BVP to elaborate the numerical shooting approach.

$$\left.\begin{aligned} &f'''(\eta) = -Af(\eta)f''(\eta) - Bf'^2(\eta) \\ &f(0) = \alpha,\ f'(0) = \gamma,\ f'(\infty) = 0. \end{aligned}\right\} \tag{2.1}$$

To reduce the order of the above boundary value problem, introduce the following notations.

$$f = Y_1 \quad f' = Y_1' = Y_2 \quad f'' = Y_2' = Y_3, \quad f''' = Y_3'. \tag{2.2}$$

As a result, (2.1) is converted into the following set of first order ODEs.

$$Y_1' = Y_2, \qquad Y_1(0) = \alpha, \tag{2.3}$$

$$Y_2' = Y_3, \qquad Y_2(0) = \gamma, \tag{2.4}$$

$$Y_3' - AY_1Y_3 - BY_2^2, \qquad Y_3(0) = r. \tag{2.5}$$

where r is the missing initial condition. The RK-4 approach will be used to numerically solve the IVP mentioned above. The missing condition r is to be selected such that:

$$Y_2(\infty, r) = 0. \tag{2.6}$$

For convenience, now onward $Y_2(\infty, r)$ will be denoted by $Y_2(r)$. Let us further denote $Y_2(r) - 0$ by $H(r)$, so that

$$H(r) = 0. \tag{2.7}$$

The above non-linear algebraic eqaution will be solved by Newton's technique. This method takes the following iterative formula.

$$\begin{aligned} r^{n+1} &= r^n - \frac{H(r^n)}{\frac{\partial H(r^n)}{\partial r}}, \\ \Rightarrow \quad r^{n+1} &= r^n - \frac{Y_2(r^n) - 0}{\frac{\partial Y_2(r^n)}{\partial r}}. \end{aligned} \tag{2.8}$$

To find $\dfrac{\partial Y_2(r^n)}{\partial r}$, the following notations are introduced.

$$\frac{\partial Y_1}{\partial r} = Y_4, \quad \frac{\partial Y_2}{\partial r} = Y_5, \quad \frac{\partial Y_3}{\partial r} = Y_6. \tag{2.9}$$

The Newton's iterative technique will acquire the following form as a result of these new notations.

$$r^{n+1} = r^n - \frac{Y_2(r^n) - 0}{Y_5(r^n)}. \tag{2.10}$$

Now differentiating the system of two first order ODEs (2.4)-(2.7) w.r.t r, we get new set of ODEs, as follows.

$$Y_4' = Y_5, \qquad Y_4(0) = 0. \tag{2.11}$$

$$Y_5' = Y_6, \qquad Y_5(0) = 0, \tag{2.12}$$

$$Y_6' - A(Y_1Y_6 + Y_4Y_3) - 2BY_2Y_5, \qquad Y_6(0) = 1. \tag{2.13}$$

Writing all the four ODEs (2.3), (2.4), (2.11) and (2.12) together, following IVP is obtained.

$$\begin{aligned}
Y_1' &= Y_2, & Y_1(0) &= \alpha. \\
Y_2' &= Y_3, & Y_2(0) &= \gamma. \\
Y_3' &= -AY_1Y_3 - BY_2^2, & Y_3(0) &= r. \\
Y_4' &= Y_5, & Y_4(0) &= 1. \\
Y_5' &= Y_6, & Y_5(0) &= 0. \\
Y_6' &= -A(Y_1Y_6 + Y_4Y_3) - 2BY_2Y_5, & Y_6(0) &= 1.
\end{aligned}$$

Runge-Kutta method of order four will be used to solve the above IVP. The missing condition will be obtained by Newton method and the stopping criteria for this technique is as follows,

$$\mid Y_2(r) - 0 \mid < \epsilon,$$

where $\epsilon > 0$ is a random small positive number.

Chapter 3

MHD Thermal Boundary Layer Flow of a Casson Fluid on a Stretching Wedge

3.1 Introduction

In this chapter, magneto hydrodynamics (MHD) thermal boundary layer flow of Casson fluid over a stretching penetrable wedge with convective boundary condition and ohmic heating by Hussain et al.[27] is examined. In this article, the BVP is solved through HAM method. The flow problem contains two dimensional continuity, momentum and energy equations. In which momentum and energy equations are coupled equations. PDEs are transformed into ODEs by using given similarity transformations [12].

This obtained BVP is numerically solved by shooting method. Furthermore, the results are validated by inbuilt command bvp4c of the MATLAB. At the end of this chapter, impact of physical parameters over velocity profile $f'(\eta)$ and temperature profile $\theta(\eta)$ are described through tables and graphs.

3.2 Mathematical Models

Figure 3.1 shows electrically conducting thermal radiative 2D mixed convective Casson fluild flow on stretching wedge. The cartesian coordinates are denoted by (x, y) from which x-direction is along with the wedge and y-direction is normal to the wedge. The stretcching velocity of wedge is represented by U_w and the

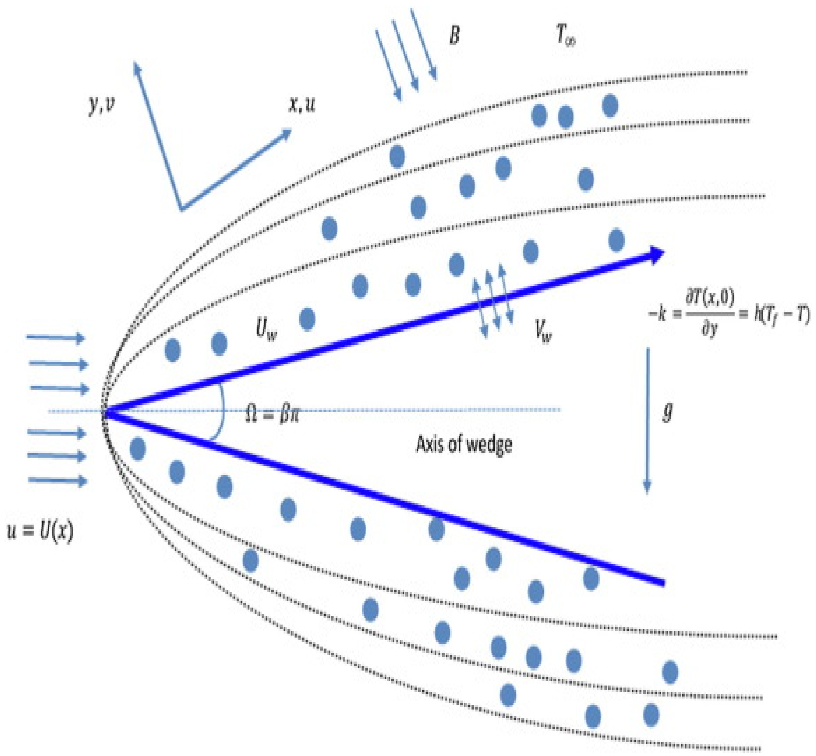

Figure 3.1: Geometry of the problem.

velocity which is distant from the wedge is U which depends on x i.e $U = U_o x_m$. The stretching wedge has suction and injection velocity which is denoted by v_w. During the heating of the wedge, a hot fluid with temperature T_f produces a high heat transfer coefficient h_f, where T_∞ is the temperature of the fluid away from the wedge. The uniform magnetic field is denoted by B which is acting along y-direction and is equivalent to $B = B_o x^{\frac{m-1}{2}}$. The wedge angle is denoted by $\Omega = \beta\pi$.

3.3 Governing Equations

The Governing model of the problem is presented below:

$$\frac{\partial u}{\partial x}+\frac{\partial v}{\partial y}=0, \tag{3.1}$$

$$u\frac{\partial u}{\partial x}+v\frac{\partial u}{\partial y}=U\frac{dU}{dx}+\nu\Big(1+\frac{1}{\delta}\Big)\frac{\partial^2 u}{\partial y^2}+g\beta_o\big(T-T_\infty\big)Sin\frac{\Omega}{2}-\frac{\sigma B^2}{\rho}\big(u-U\big), \tag{3.2}$$

$$\rho c_p\Big(u\frac{\partial T}{\partial x}+v\frac{\partial T}{\partial y}\Big)=-u\Big(\rho U\frac{dU}{dx}+\sigma B^2 U\Big)+\alpha\frac{\partial^2 T}{\partial y^2}-\frac{\partial q_r}{\partial y}+\sigma B^2 u^2. \tag{3.3}$$

Boundary conditions of the given problem are given as:

$$u\big(x,0\big)=RU, \tag{3.4}$$

$$v\big(x,0\big)=v_w=-\big(vU_o\big)^{\frac{1}{2}}C\Big(\frac{m+1}{2}\Big)x^{\frac{m+1}{2}}, \tag{3.5}$$

$$\frac{\partial T\big(x,0\big)}{\partial y}=\frac{h}{k}\big(T-T_f\big), \tag{3.6}$$

$$u\big(x,\infty_n\big)\ \rightarrow\ U_o x^m,\quad T\big(x,\infty_n\big)\ \rightarrow\ T_{\infty_n}. \tag{3.7}$$

Here, ν, g, β_o, σ, ρ, c_p, α denotes the kinematic viscosity, gravity field, coefficient of thermal expansion, conductivity of fluid due to electric current, fluid density, heat capacity, thermal conductivity. The term $\frac{\partial q_r}{\partial y}$ here q_r is radiative heat flux and is equal to -$\frac{4\sigma_o}{3k^*}\frac{\partial T^4}{\partial y}$, σ_o and k^* are known as Stefan-Boltzman constant and the mean absorption coefficient respectively.

$$q_r=-\frac{4\sigma_o}{3k^*}\frac{\partial T^4}{\partial y}. \tag{3.8}$$

The Taylor series expansion on function taken as T^4 about T_∞ is as follows:

$$T^4=T_\infty^4+\frac{4T_\infty^3\big(T-T_\infty\big)}{1!}+\frac{12T_\infty^2\big(T-T_\infty\big)^2}{2!}+...,$$
$$T^4=T_\infty^4+4T_\infty^3\big(T-T_\infty\big)+6T_\infty^2\big(T-T_\infty\big)^2+...$$

The higher order derivatives are neglected because of the temperature difference in the fluid is too small. Hence, the value of T^4 is:

$$
\begin{aligned}
&T^4 = T_\infty^4 + 4T_\infty^3 T - 4T_\infty^4,\\
&T^4 = 4T_\infty^3 T - 3T_\infty^4,\\
&\frac{\partial T^4}{\partial y} = 4T_\infty^3 \frac{\partial T}{\partial y}.
\end{aligned}
\tag{3.9}
$$

Now the final form of q_r is obtained by using (3.9) in (3.8)

$$
q_r = -\frac{16\sigma_o T_\infty^3}{3k^*}\frac{\partial T}{\partial y}. \tag{3.10}
$$

The following transformations are used to convert the PDEs into non-dimensional form:

$$
\begin{aligned}
&= \sqrt{U\nu x} f,\\
u &= \frac{\partial \psi}{\partial y},\\
v &= -\frac{\partial \psi}{\partial x},\\
\eta &= \sqrt{\frac{U_o}{\nu}} x^{\frac{m-1}{2}} y,\\
\theta(\eta) &= \frac{T - T_\infty}{T_f - T_\infty}.
\end{aligned}
$$

Where ψ is the stream function and u and v are the velocity components along x-axis and y-axis. By using stream function, values of u and v are found. Moreover, velocities u,v and temperuatue T depends on η variable.

3.4 Dimensionless Equations

Following calculations are done for computing the expression for u and v:

$$
\begin{aligned}
u &= \frac{\partial \psi}{\partial y},\\
u &= \sqrt{U_o \nu}\Big[f \frac{\partial x^{\frac{m+1}{2}}}{\partial y} + x^{\frac{m+1}{2}} \frac{\partial f}{\partial y}\Big],
\end{aligned}
$$

$$u = \sqrt{U_o\nu}\Big[x^{\frac{m+1}{2}}f'(\eta)\frac{\partial\eta}{\partial y}\Big],$$
$$u = \sqrt{U_o\nu}\Big[x^{\frac{m+1}{2}}f'(\eta)\frac{\sqrt{U_o}}{\sqrt{\nu}}x^{\frac{m-1}{2}}\Big],$$
$$u = U_o x^m f'(\eta). \tag{3.11}$$
$$v = -\frac{\partial\psi}{\partial x},$$
$$v = -\sqrt{U_o\nu}\Big[f\frac{\partial x^{\frac{m+1}{2}}}{\partial x} + x^{\frac{m+1}{2}}f'(\eta)\frac{\partial\eta}{\partial x}\Big],$$
$$v = -\sqrt{U_o\nu}\Big[\frac{m+1}{2}fx^{\frac{m-1}{2}} + x^{\frac{m-1}{2}}f'(\eta)\frac{m-1}{2}\eta\Big],$$
$$v = -\sqrt{U_o\nu}x^{\frac{m-1}{2}}\Big[\frac{m+1}{2}f + f'(\eta)\frac{m-1}{2}\eta\Big]. \tag{3.12}$$

Substituting values (3.11) and (3.12) in L.H.S of (3.1) we get:

$$\frac{\partial u}{\partial x} + \frac{\partial v}{\partial y} = 0,$$
$$\frac{\partial u}{\partial x} = \frac{\partial\big(U_o x^m f'\big)}{\partial x},$$
$$= U_o\Big[f'\frac{\partial x^m}{\partial x} + x^m f''\eta\frac{\partial\eta}{\partial x}\Big],$$
$$= U_o\Big[f' m x^{m-1} + x^m f''(\eta)\sqrt{\frac{U_o}{\nu}}y\frac{m-1}{2}x^{\frac{m-3}{2}}\Big],$$
$$\frac{\partial u}{\partial x} = mU_o f' x^{m-1} + U_o\sqrt{\frac{U_o}{\nu}}f''\frac{m-1}{2}x^{\frac{3(m-1)}{2}}. \tag{3.13}$$
$$\frac{\partial v}{\partial y} = \frac{\partial}{\partial y}\Big[-\sqrt{U_o\nu}x^{\frac{m-1}{2}}\frac{m+1}{2}f - \sqrt{U_o\nu}x^{\frac{m-1}{2}}\frac{m-1}{2}\eta f'\Big],$$
$$= -\sqrt{U_o\nu}\Big[\frac{m+1}{2}f\frac{\partial x^{\frac{m-1}{2}}}{\partial y} + \frac{m+1}{2}x^{\frac{m-1}{2}}f'\sqrt{\frac{U_o}{\nu}}x^{\frac{m-1}{2}}\Big] -$$
$$\sqrt{U_o\nu}\Big[\frac{m-1}{2}f'\frac{\partial x^{\frac{m-1}{2}}}{\partial y}\eta + \frac{m-1}{2}x^{\frac{m-1}{2}}f'\frac{\partial\eta}{\partial y} + \frac{m-1}{2}\eta f''\frac{\partial\eta}{\partial y}\Big],$$
$$= -\sqrt{U_o\nu}\Big[\frac{m+1}{2}x^{\frac{m-1}{2}}f'\sqrt{\frac{U_o}{\nu}}x^{\frac{m-1}{2}} +$$
$$\frac{m-1}{2}x^{\frac{m-1}{2}}f'\sqrt{\frac{U_o}{\nu}}x^{\frac{m-1}{2}} + \frac{m-1}{2}x^{\frac{m-1}{2}}\eta f''\sqrt{\frac{U_o}{\nu}}x^{\frac{m-1}{2}}\Big],$$
$$= -U_o x^{m-1}\Big[\frac{m+1}{2}f' + \frac{m-1}{2}f' + \frac{m-1}{2}\eta f''\Big],$$
$$\frac{\partial v}{\partial y} = -U_o x^{m-1}\Big[mf' + \frac{m-1}{2}\eta f''\Big]. \tag{3.14}$$

Putting equations (3.13) and (3.14) in (3.1) then we get:

$$\frac{\partial u}{\partial x}+\frac{\partial v}{\partial y}=mU_of'x^{m-1}+U_o\sqrt{\frac{U_o}{\nu}}f''\frac{m-1}{2}x^{\frac{3(m-1)}{2}}-U_ox^{m-1}\Big[mf'+\frac{m-1}{2}\eta f''\Big],$$
$$=U_o\sqrt{\frac{U_o}{\nu}}f''\frac{m-1}{2}x^{\frac{3(m-1)}{2}}-U_o\sqrt{\frac{U_o}{\nu}}f''x^{\frac{3(m-1)}{2}}\frac{m-1}{2},$$
$$=0.$$

Above result shows that continuity equation is satisfied by given transformations. Now dimensional momentum equation is converted into non-dimensional form by using following derivatives

$$v\frac{\partial u}{\partial y}=\Big[-\sqrt{U_o\nu}x^{\frac{m-1}{2}}\frac{m+1}{2}f-\sqrt{U_o\nu}x^{\frac{m-1}{2}}\frac{m-1}{2}\eta f'\Big]\Big[\frac{U_o\sqrt{U_o}}{\sqrt{\nu}}f''x^{\frac{3m-1}{2}}\Big],$$
$$v\frac{\partial u}{\partial y}=-U_o^2x^{2m-1}\frac{m+1}{2}ff''-U_o^2x^{2m-1}\frac{m-1}{2}\eta f'f''. \tag{3.15}$$
$$\frac{dU}{dx}=mU_ox^{m-1}, \tag{3.16}$$
$$U\frac{dU}{dx}=mU_o^2x^{2m-1}. \tag{3.17}$$

Taking second derivative of $\dfrac{\partial u}{\partial y}$:

$$\frac{\partial^2u}{\partial y^2}=\frac{\partial}{\partial y}\Big[\frac{U_o\sqrt{U_o}}{\sqrt{\nu}}x^{\frac{3m-1}{2}}f''\Big],$$
$$=\frac{U_o\sqrt{U_o}}{\sqrt{\nu}}\Big[f''\frac{\partial}{\partial y}x^{\frac{3m-1}{2}}+x^{\frac{3m-1}{2}}f'''\frac{\partial\eta}{\partial y}\Big],$$
$$=\frac{U_o\sqrt{U_o}}{\sqrt{\nu}}\Big[x^{\frac{3m-1}{2}}f'''\sqrt{\frac{U_o}{\nu}}x^{\frac{m-1}{2}}\Big],$$
$$\frac{\partial^2u}{\partial y^2}=\frac{U_o^2}{\nu}x^{2m-1}f'''. \tag{3.18}$$
$$g\beta_o\big(T-T_\infty\big)Sin\frac{\Omega}{2}=g\beta_o\theta(\eta)\big(T_f-T_\infty\big)Sin\frac{\Omega}{2}. \tag{3.19}$$
$$\frac{\sigma B^2}{\rho}\big(u-U\big)=\frac{\sigma B^2}{\rho}\big(Uf'-U\big). \tag{3.20}$$

Now put the related terms of momentum equation in (3.2).

$$u\frac{\partial u}{\partial x}+v\frac{\partial u}{\partial y}=mU_o^2x^{2m-1}f'^2+\frac{U_o^2\sqrt{U_o}}{\sqrt{\nu}}\frac{m-1}{2}yx^{\frac{5m-3}{2}}f'f''-U_o^2x^{2m-1}\frac{m+1}{2}ff''-$$
$$U_o^2x^{2m-1}\frac{m-1}{2}\eta f'f'',$$

$$u\frac{\partial u}{\partial x}+v\frac{\partial u}{\partial y}=mU_o^2x^{2m-1}f'^2+U_o^2\frac{m-1}{2}x^{2m-1}\eta f'f''-U_o^2x^{2m-1}\frac{m+1}{2}ff''-$$
$$U_o^2x^{2m-1}\frac{m-1}{2}\eta f'f''. \tag{3.21}$$

Now considering the R.H.S of the momentum equation

$$U\frac{dU}{dx}+\nu\Big(1+\frac{1}{\delta}\Big)\frac{\partial^2 u}{\partial y^2}+g\beta_o\big(T-T_\infty\big)Sin\frac{\Omega}{2}-\frac{\sigma B^2}{\rho}\big(u-U\big)=mU_o^2x^{2m-1}+$$
$$\nu\Big(1+\frac{1}{\delta}\Big)\frac{U_o^2}{\nu}x^{2m-1}f'''+g\beta_o\theta(\eta)\big(T_f-T_\infty\big)Sin\frac{\Omega}{2}-\frac{\sigma B^2}{\rho}\big(U_ox^mf'-U_ox^m\big),$$
$$U\frac{dU}{dx}+\nu\Big(1+\frac{1}{\delta}\Big)\frac{\partial^2 u}{\partial y^2}+g\beta_o\theta(\eta)\big(T_f-T_\infty\big)Sin\frac{\Omega}{2}-\frac{\sigma B^2}{\rho}\big(u-U\big)=$$
$$mU_o^2x^{2m-1}+U_o^2x^{2m-1}\Big(1+\frac{1}{\delta}\Big)f'''+g\beta_o\theta\big(T_f-T_\infty\big)Sin\frac{\Omega}{2}-x^{2m-1}MU_o^2\big(f'-1\big). \tag{3.22}$$

$$M=\frac{\sigma B_o^2}{\rho U_o}$$

Equilating (3.21) and (3.22):

$$U_o^2x^{2m-1}\Big[mf'^2-\frac{m+1}{2}ff''\Big]=U_o^2x^{2m-1}\Big[m+\Big(1+\frac{1}{\delta}\Big)f'''+\lambda Sin\frac{\Omega}{2}\theta-M\big(f'-1\big)\Big],$$
$$f'''\Big(1+\frac{1}{\delta}\Big)+\Big(\frac{m+1}{2}\Big)ff''+\big(1-f'^2\big)m-M\big(f'-1\big)+\lambda Sin\frac{\Omega}{2}\theta=0,$$
$$f'''=\Big(1+\frac{1}{\delta}\Big)\Big[-\frac{m+1}{2}ff''-m+mf'^2+Mf'-M-\lambda Sin\frac{\Omega}{2}\theta\Big]. \tag{3.23}$$

Following parameters are used in above equations for changing them from dimensional to non-dimensional equations:
$M=\frac{\sigma B_o^2}{\rho U_o}$, $\lambda=\frac{Gr_x}{Re_x^2}$ where $Gr_x=\frac{g\beta_o(T_f-T_\infty)x^3}{\nu^2}$, $Re_x=\frac{Ux}{\nu}$.
Some more derivatives are calculated below for conversion of energy equation

$$\theta(\eta)=\frac{T-T_\infty}{T_f-T_\infty},$$
$$T=\big(T_f-T_\infty\big)\theta(\eta)+T_\infty. \tag{3.24}$$

Diferentiate both sides of (3.24) w.r.t. x:

$$\frac{\partial T}{\partial x}=\big(T_f-T_\infty\big)\theta'(\eta)\frac{\partial \eta}{\partial x},$$

$$\frac{\partial T}{\partial x} = (T_f - T_\infty)\theta'(\eta)\sqrt{\frac{U_o}{\nu}}\frac{m-1}{2}x^{\frac{m-3}{2}}y, \tag{3.25}$$

$$u\frac{\partial T}{\partial x} = \frac{U_o\sqrt{U_o}}{\nu}\Big(\frac{m-1}{2}\Big)(T_f - T_\infty)yx^{\frac{3m-3}{2}}f'\theta'. \tag{3.26}$$

Differentiate both sides of (3.24) w.r.t. y:

$$\frac{\partial T}{\partial y} = (T_f - T_\infty)\theta'(\eta)\frac{\partial \eta}{\partial y},$$

$$\frac{\partial T}{\partial y} = (T_f - T_\infty)\theta'(\eta)\sqrt{\frac{U_o}{\nu}}x^{\frac{m-1}{2}}, \tag{3.27}$$

$$v\frac{\partial T}{\partial y} = \Big[-\sqrt{U_o\nu}x^{\frac{m-1}{2}}\Big(\frac{m+1}{2}f + f'(\eta)\frac{m-1}{2}\eta\Big)\Big]\Big[(T_f - T_\infty)\theta'(\eta)\sqrt{\frac{U_o}{\nu}}x^{\frac{m-1}{2}}\Big],$$

$$v\frac{\partial T}{\partial y} = -U_o x^{m-1}\Big(\frac{m+1}{2}\Big)(T_f - T_\infty)\theta' f - U_o x^{m-1}\Big(\frac{m-1}{2}\Big)(T_f - T_\infty)\theta' f'\eta. \tag{3.28}$$

Multiply $-u$ and ρ with (3.17), we will get:

$$-u\rho U\frac{dU}{dx} = -\rho m U_o^3 x^{3m-1}f'. \tag{3.29}$$

$$\sigma B^2 U = \sigma B_o^2 x^{m-1}U_o x^m,$$

$$= \sigma B_o^2 U_o x^{2m-1},$$

$$-u\sigma B^2 U = -\sigma B_o^2 U_o^2 x^{3m-1}f'. \tag{3.30}$$

Taking second derivative of $\frac{\partial T}{\partial y}$:

$$\frac{\partial^2 T}{\partial y^2} = \frac{\partial}{\partial y}\Big[(T_f - T_\infty)\theta'\sqrt{\frac{U_o}{\nu}}x^{\frac{m-1}{2}}\Big],$$

$$= (T_f - T_\infty)\sqrt{\frac{U_o}{\nu}}\Big[\theta''\frac{\partial \eta}{\partial y}x^{\frac{m-1}{2}} + \theta'\frac{\partial x^{\frac{m-1}{2}}}{\partial y}\Big],$$

$$\frac{\partial^2 T}{\partial y^2} = (T_f - T_\infty)\frac{U_o}{\nu}\theta'' x^{m-1}, \tag{3.31}$$

$$\alpha\frac{\partial^2 T}{\partial y^2} = \alpha(T_f - T_\infty)\frac{U_o}{\nu}\theta'' x^{m-1}. \tag{3.32}$$

Now take the derivative of (3.10) w.r.t. y:

$$\frac{\partial q_r}{\partial y} = -\frac{16\sigma_o T_\infty^3}{3k^*}\frac{\partial^2 T}{\partial y^2},$$

$$\frac{\partial q_r}{\partial y} = -\frac{16\sigma_o T_\infty^3}{3k^*}\big(T_f - T_\infty\big)\frac{U_o}{\nu}\theta'' x^{m-1}. \tag{3.33}$$

$$\sigma B^2 u^2 = \sigma\big(B_o^2 x^{m-1}\big)\big(U_o^2 x^{2m}\big(f'\big)^2\big),$$

$$\sigma B^2 u^2 = \sigma B_o^2 x^{3m-1} U_o^2\big(f'\big)^2. \tag{3.34}$$

$$u\frac{\partial T}{\partial x} + v\frac{\partial T}{\partial y} = \frac{U_o\sqrt{U_o}}{\nu}\Big(\frac{m-1}{2}\Big)\big(T_f - T_\infty\big)yx^{\frac{3m-3}{2}} f'\theta' - U_o x^{m-1}\Big(\frac{m+1}{2}\Big)$$

$$\big(T_f - T_\infty\big)\theta' f - U_o x^{m-1}\Big(\frac{m-1}{2}\Big)\big(T_f - T_\infty\big)\theta' f'\eta,$$

$$u\frac{\partial T}{\partial x} + v\frac{\partial T}{\partial y} = -U_o x^{m-1}\frac{m+1}{2}\big(T_f - T_\infty\big)f\theta'. \tag{3.35}$$

$$-u\Big(\rho U\frac{dU}{dx} + \sigma B^2 U\Big) + \alpha\frac{\partial^2 T}{\partial y^2} - \frac{\partial q_r}{\partial y} + \sigma B^2 u^2 = -\frac{1}{c_p} m U_o^3 x^{3m-1} f' -$$

$$\frac{\sigma}{\rho c_p} B_o^2 U_o^2 x^{3m-1} f' + \frac{\alpha}{\rho c_p}\big(T_f - T_\infty\big)\frac{U_o}{\nu}x^{m-1}\theta'' + \frac{16\sigma_o T_\infty^3}{3k^*}\big(T_f - T_\infty\big)\frac{U_o}{\nu}\theta'' x^{m-1} +$$

$$\frac{\sigma}{\rho c_p} B_o^2 x^{3m-1} U_o^2\big(f'\big)^2. \tag{3.36}$$

Comparing (3.35) and (3.36):

$$-U_o x^{m-1}\Big[\frac{m+1}{2}\big(T_f - T_\infty\big)f\theta'\Big] = U_o x^{m-1}\Big[-\frac{1}{c_p} m U_o^2 x^{2m} f' - \frac{\sigma}{\rho c_p} B_o^2 U_o x^{2m} f' +$$

$$\frac{\alpha}{\rho c_p \nu}\big(T_f - T_\infty\big)\theta'' + \frac{16\sigma_o T_\infty^3}{\nu\rho c_p 3k^*}\big(T_f - T_\infty\big)\theta'' + \frac{\sigma}{\rho c_p} B_o^2 x^{2m} U_o\big(f'\big)^2\Big],$$

$$-\Big(\frac{m+1}{2}\Big)\theta' f = -\frac{1}{c_p\big(T_f - T_\infty\big)} m U_o^2 x^{2m} f' - \frac{\sigma}{\rho c_p\big(T_f - T_\infty\big)} B_o^2 U_o x^{2m} f' +$$

$$\frac{\alpha}{\rho c_p \nu}\theta'' + \frac{16\sigma_o T_\infty^3}{\nu\rho c_p 3k^*}\theta'' + \frac{\sigma}{\rho c_p\big(T_f - T_\infty\big)} B_o^2 x^{2m} U_o\big(f'\big)^2\Big],$$

$$-\Big(\frac{m+1}{2}\Big)\theta' f = -\frac{1}{c_p\big(T_f - T_\infty\big)} m U^2 f' - \frac{\sigma}{\rho c_p\big(T_f - T_\infty\big)} B_o^2 U_o x^{2m} f' +$$

$$\frac{\alpha}{c_p\mu}\Big[1 + Nr\Big]\theta'' + \frac{\sigma}{\rho c_p\big(T_f - T_\infty\big)} B_o^2 x^{2m} U_o\big(f'\big)^2,$$

$$\frac{\alpha}{c_p\mu}\Big[1 + Nr\Big]\theta'' + \Big(\frac{m+1}{2}\Big)\theta' f - \frac{1}{c_p\big(T_f - T_\infty\big)} m U^2 f' - \frac{\sigma}{\rho c_p\big(T_f - T_\infty\big)} B_o^2 U_o x^{2m} f' +$$

$$\frac{\sigma}{\rho c_p\big(T_f - T_\infty\big)} B_o^2 x^{2m} U_o\big(f'\big)^2 = 0,$$

Multiply above euquation with $\frac{\mu c_p}{\alpha}$ we get:

$$\begin{aligned}
&\Big[1+Nr\Big]\theta''+\frac{\mu c_p}{\alpha}\Big(\frac{m+1}{2}\Big)f\theta'-\frac{mU^2\mu}{\alpha\big(T_f-T_\infty\big)}f'-\frac{\sigma B_o^2U_ox^{2m}\mu}{\alpha\rho\big(T_f-T_\infty\big)}f'+\\
&\frac{\sigma B_o^2U_ox^{2m}\mu}{\alpha\rho\Big(T_f-T_\infty\Big)}f'^2=0,\\
&\Big[1+Nr\Big]\theta''+Pr\Big(\frac{m+1}{2}\Big)f\theta'-mEcPrf'-MEcPrf'+EcPrMf'^2=0,\\
&\theta''=\frac{1}{\big(1+Nr\big)}\Big[-Pr\Big(\frac{m+1}{2}\Big)f\theta'+mEcPrf'+MEcPrf'-MEcPrf'^2\Big].
\end{aligned} \tag{3.37}$$

using the following parameters are used in above equations:

$$Nr=\frac{16T_\infty^3\sigma_o}{3k^*\alpha},\qquad Ec=\frac{U^2}{c_p(T_f-T_\infty)}\quad \text{and}\quad Pr=\frac{\mu c_p}{\alpha}$$

Detailed conversion of BCs are as follows:

$$\begin{aligned}
&u(x,0)=RU,\\
&U_ox^mf'(0)=RU_ox^m,\quad Using,\quad u=U_ox^mf'(\eta)\quad and\quad U=U_ox^m\\
&f'(0)=R.\\
&v(x,0)=v_w=-\sqrt{U_o\nu}C\sqrt{\frac{m+1}{2}}x^{\frac{m-1}{2}},\\
&v(x,0)=-\sqrt{U_o\nu}x^{\frac{m-1}{2}}\sqrt{\frac{m+1}{2}}f(0)-\sqrt{U_o\nu}\sqrt{\frac{m+1}{2}}\eta f'(0),\quad using\quad (3.12)\\
&v(x,0)=-\sqrt{U_o\nu}x^{\frac{m-1}{2}}\sqrt{\frac{m+1}{2}}f(0),\\
&v(x,0)=v_w,\\
&-\sqrt{U_o\nu}x^{\frac{m-1}{2}}\sqrt{\frac{m+1}{2}}f(0)=-\sqrt{U_o\nu}x^{\frac{m-1}{2}}\Big(\frac{m+1}{2}\Big),\\
&f(0)=C.\\
&\frac{\partial}{\partial y}T(x,0)=\frac{h}{k}\big(T-T_f\big),\\
&(T_f-T_\infty)\theta'(0)\sqrt{\frac{U_o}{\nu}}x^{\frac{m-1}{2}}=\frac{h}{k}\Big[T_\infty+\big(T_f-T_\infty\big)\theta(0)-T_f\Big],\quad using\quad (3.27)\\
&(T_f-T_\infty)\theta'(0)\sqrt{\frac{U_o}{\nu}}x^{\frac{m-1}{2}}=\frac{h}{k}\big[\Big(T_f-T_\infty\big)\theta(0)-\big(T_f-T_\infty\Big)\Big],\\
&\theta'(0)\sqrt{\frac{U_o}{\nu}}x^{\frac{m-1}{2}}=\frac{h}{k}\big(\theta(0)-1\big),
\end{aligned}$$

$$\theta'(0) = \frac{h}{k}\sqrt{\frac{\nu}{U_o}}x^{\frac{1-m}{2}}\big(\theta(0)-1\big),$$
$$\theta'(0) = \frac{h}{k}\sqrt{\frac{\nu x}{U_o x^m}}\big(\theta(0)-1\big),$$
$$\theta'(0) = \frac{h}{k}\sqrt{\frac{\nu x}{U}}\big(\theta(0)-1\big),$$
$$\theta'(0) = B_i\ \big(\theta(0)-1\big),$$
$$\theta'(0) = -B_i\ \big(1-\theta(0)\big).\ \ Here,\ \ B_i = \frac{h}{k}\sqrt{\frac{\nu x}{U}}.$$
$$u(x,\infty) = U_o x^m,$$
$$U_o x^m f'(\infty) = U_o x^m,\ \ Since,\ \ u = U_o x^m f'(\eta)$$
$$f'(\infty) = 1.$$
$$T(x,\infty) = T(\infty),$$
$$\theta(\infty)(T_f - T_\infty) + T_\infty = T(\infty),$$
$$\theta(\infty)(T_f - T_\infty) = 0,$$
$$T_f - T_\infty \neq 0,$$
$$\theta(\infty) = 0.$$

The dimensional form of skin friction and Nusselt number is:

$$C_f = \frac{\left(\mu_\beta + \frac{p_y}{\sqrt{2\pi}}\right)\frac{\partial u}{\partial y}|_{y=0}}{\rho U^2},$$
$$Nu_x = \frac{x q_w}{\alpha\big(T_f - T_\infty\big)}.$$

Here, the dimensional formula of surface drag force and Nusselt Number is converted into dimensionless form which is given below:

$$C_f = \frac{\mu_\beta\left(1 + \frac{p_y}{\mu_\beta\sqrt{2\pi}}\right)\frac{\partial u}{\partial y}|_{y=0}}{\rho U^2},$$
$$C_f = \frac{\mu_\beta\left(1 + \frac{p_y}{\mu_\beta\sqrt{2\pi}}\right)U_o\sqrt{U_o}x^{\frac{3m-1}{2}}f''(0)}{\sqrt{\nu}\rho U_o^2 x^{2m}},$$
$$C_f = \frac{\mu_\beta\left(1 + \frac{p_y}{\mu_\beta\sqrt{2\pi}}\right)f''(0)}{\rho\sqrt{\nu}\sqrt{U_o x^m x}},$$

$$
\begin{aligned}
C_f &= \frac{\nu\left(1+\frac{1}{\delta}\right)f''(0)}{\sqrt{\nu}\sqrt{Ux}},\\
C_f &= \frac{\left(1+\frac{1}{\delta}\right)f''(0)}{(Re_x)^{\frac{1}{2}}},\\
(Re_x)^{\frac{1}{2}}C_f &= \left(1+\frac{1}{\delta}\right)f''(0).\\
Nu_x &= \frac{xq_w}{\alpha(T_f-T_\infty)},\\
Nu_x &= \frac{-x\alpha\frac{\partial T}{\partial y}|_{y=0}}{\alpha(T_f-T_\infty)},\\
Nu_x &= \frac{-x(T_f-T_\infty)\theta'(0)x^{\frac{m-1}{2}}\frac{\sqrt{U_o}}{\sqrt{\nu}}}{(T_f-T_\infty)},\\
Nu_x &= -\theta'(0)\frac{\sqrt{U_o x^m x}}{\sqrt{\nu}},\\
Nu_x &= -\theta'(0)\frac{\sqrt{Ux}}{\sqrt{\nu}},\\
(Re_x)^{\frac{-1}{2}}Nu_x &= -\theta'(0).
\end{aligned}
$$

Final form of dimensionless momentum and energy equations are given below:

$$
f''' = \left(1+\frac{1}{\delta}\right)\Big[-\frac{m+1}{2}ff''-m+mf'^2+Mf'-M-\lambda Sin\frac{\Omega}{2}\theta\Big], \tag{3.38}
$$

$$
\theta'' = \frac{1}{\left(1+Nr\right)}\Big[-Pr\Big(\frac{m+1}{2}\Big)f\theta'+mEcPrf'+MEcPrf'-MEcPrf'^2\Big]. \tag{3.39}
$$

Along with BCs.:

$$
\left.
\begin{aligned}
\theta'(0) &= -B_i + B_i\,\theta(0),\ \theta(\infty_n)=0.\\
f(0)=C,\ & f'(0)=R,\ f'(\infty_n)=1.
\end{aligned}
\right\} \tag{3.40}
$$

3.5 Shooting Method

Now the shooting method is applied on BVP given by (3.38) and (3.39) along with boundary conditions (3.40). Using the following notation so that BVP is converted into an initial value problem.

$$
\begin{aligned}
f &= y_1, \\
f' &= y_1' = y_2, \\
f'' &= y_2' = y_3, \\
f''' &= y_3', \\
\theta &= y_4, \\
\theta' &= y_4' = y_5, \\
\theta'' &= y_5'.
\end{aligned}
$$

Using the above notations (3.38) and (3.39) are transformed into five first order differential equations

$$
\begin{aligned}
& y_1' = y_2 \quad ; && y_1(0) = C, \\
& y_2' = y_3 \quad ; && y_2(0) = R, \quad y_2(\infty) = 1, \\
& y_3' = \frac{1}{\left(1+\frac{1}{\delta}\right)}\Big[-\Big(\frac{m+1}{2}\Big)y_1y_3 - m + my_2^2 + My_2 - M - \lambda Sin\frac{\Omega}{2}y_4\Big], && y_3(0) = s, \\
& y_4' = y_5, \quad ; && y_4(0) = q, \quad y_4(\infty) = 0, \\
& y_5' = \frac{1}{(1+Nr)}\Big[-Pr\Big(\frac{m+1}{2}\Big)y_1y_5 + mEcPry_2 + MEcPry_2 - MEcPry_2^2\Big], && \\
& && y_5(0) = -Bi(1-q).
\end{aligned}
$$

Where s and q are the missing initial conditions. Now the above first order initial value problem is solved by using Runge-Kutta technique. The initial missing conditions are to be selected such as:

$$
y_2(\infty_n, s, q) = 1, \quad y_4(\infty_n, s, q) = 0.
$$

Denote

$$
\begin{aligned}
\phi_1(s,q) &= y_2(\infty_n, s, q) - 1, \\
\phi_2(s,q) &= y_4(\infty_n, s, q).
\end{aligned}
$$

If $\phi_1(s,q) = 0$ and $\phi_2(s,q) = 0$ then we get our solution, if not we apply Newton's Raphson technique to refine the following iterative formula:

$$\begin{bmatrix} s \\ q \end{bmatrix}_{(n+1)} = \begin{bmatrix} s \\ q \end{bmatrix}_{n} - \begin{bmatrix} \frac{\partial y_2}{\partial s} & \frac{\partial y_2}{\partial q} \\ \frac{\partial y_4}{\partial s} & \frac{\partial y_4}{\partial q} \end{bmatrix}_{n}^{-1} \begin{bmatrix} \phi_1 \\ \phi_2 \end{bmatrix}_{n}. \tag{3.41}$$

Following notations are used to calculate the new appeared derivatives:

$$\frac{\partial y_1}{\partial s} = y_6, \frac{\partial y_2}{\partial s} = y_7, \frac{\partial y_3}{\partial s} = y_8, \frac{\partial y_4}{\partial s} = y_9, \frac{\partial y_5}{\partial s} = y_{10}.$$
$$\frac{\partial y_1}{\partial q} = y_{11}, \frac{\partial y_2}{\partial q} = y_{12}, \frac{\partial y_3}{\partial q} = y_{13}, \frac{\partial y_4}{\partial q} = y_{14}, \frac{\partial y_5}{\partial q} = y_{15}.$$

We get the following equations by differentiating above IVP with respect to s and q

$$y_6' = y_7 \quad ; \qquad y_6(0) = 0,$$

$$y_7' = y_8 \quad ; \qquad y_7(0) = 0, \quad y_7(\infty) = 0,$$

$$y_8' = \frac{1}{\left(1+\frac{1}{\delta}\right)}\Big[-\Big(\frac{m+1}{2}\Big)\big(y_6y_3 + y_1y_8\big) + 2my_2y_7 + My_7 - \lambda Sin\frac{\Omega}{2}y_9\Big], y_8(0) = 1,$$

$$y_9' = y_{10} \;; \qquad y_9(0) = 0, \quad y_9(\infty) = 0,$$

$$y_{10}' = \frac{1}{(1+Nr)}\Big[-Pr\Big(\frac{m+1}{2}\Big)\big(y_6y_5 + y_1y_{10}\big) + mEcPry_7 +$$
$$MEcPry_7 - 2MEcPry_2y_7\Big], \qquad y_{10}(0) = 0.$$

$$y_{11}' = y_{12} \quad ; \qquad y_{11}(0) = 0,$$

$$y_{12}' = y_{13} \quad ; \qquad y_{12}(0) = 0, \quad y_{12}(\infty) = 0,$$

$$y_{13}' = \frac{1}{\left(1+\frac{1}{\delta}\right)}\Big[-\Big(\frac{m+1}{2}\Big)\big(y_{11}y_3 + y_1y_{13}\big) + 2my_2y_{12} + My_{12} - \lambda Sin\frac{\Omega}{2}y_{14}\Big],$$
$$y_{13}(0) = 0,$$

$$y_{14}' = y_{15} \quad ; \qquad y_{14}(0) = 1, \quad y_{14}(\infty) = 0,$$

$$y_{15}' = \frac{1}{\left(1+Nr\right)}\Big[-Pr\Big(\frac{m+1}{2}\Big)\big(y_{11}y_5 + y_1y_{15}\big) + mEcPry_{12} +$$
$$MEcPry_{12} - 2MEcPry_2y_{12}\Big], \qquad y_{15}(0) = B_i.$$

Following stopping criteria is used for Newton's method:

$$max(|\ \phi_1(\eta_\infty, s_n, q_n)\ |, |\ \phi_2(\eta_\infty, s_n, q_n)\ |) < \epsilon.$$

Here, $\epsilon = 10^{-8}$.

3.6 Results and Discussions

Table 3.1 depicts the value of skin fricktion and Nusselt number for multiple values of velocity ratio parameter R and wedge angle β. On both cases when $R < 1$ or $R > 1$, by increasing values of wedge angle parameter β, surface drag force coefficient $f''(0)$ increases. It is also observed that with the increase of β the temperature gradient coefficient of Nusselt number $|\theta'(0)|$ also increases. Shooting method is incorporated on MATLAB to obtain the numerical solutions. Furthermore, the inbuilt command bvp4c of MATLAB is used to validate the numerical results. Throughout the calculations, following values of various parameters are fixed such as $\delta = 1$, $m = 0.1$, $\lambda = 0.8$, $B_i = 5$, $M = 0$, $Nr = 1$, $Pr = 1$, $Ec = 0.5$ and $C = 1$.

TABLE 3.1: Results of $(Re_x)^{\frac{1}{2}} C_f$ and $(Re_x)^{\frac{-1}{2}} Nu_x$ for values of β.

		Shooting		*bvp4c*	
R	β	C_f	Nu_x	C_f	Nu_x
0.5	0.0	0.62835381300	0.54219079243	0.62835381429	0.54219078479
1.1		-0.14172056286	0.61199236333	-0.14172047375	0.61199348736
0.5	0.7	1.15684789931	0.55853729662	1.15684790290	0.55853729723
1.1		0.30646314943	0.62279353224	0.30646315370	0.62279353097
0.5	1	1.23479694857	0.56079908021	1.23479695325	0.56079908090
1.1		0.37371240787	0.62434482207	0.37371241671	0.62434481804

Table 3.2 depicts the values of surface drag force and Nusselt number for multiple values of velocity ratio parameter R and M is magnetic parameter. When $R < 1$, by increasing values of M, surface drag force coefficient $f''(0)$ also the values temperature gradient coefficient of Nusselt number $|\theta'(0)|$ increases. When $R > 1$, by increasing values of magnetic parameter M, surface drag force coefficient $f''(0)$ and the values of $|\theta'(0)|$ deccreases. Numerical solutions accquired by the shooting method are validated by the inbuilt command bvp4c of MATLAB.

Table 3.2: Results of $(Re_x)^{\frac{1}{2}}C_f$ and $(Re_x)^{\frac{-1}{2}}Nu_x$ for values of M.

		Shooting		*bvp4c*	
R	M	C_f	Nu_x	C_f	Nu_x
0.1	0.0	1.13512565646	0.49094927325	1.13512604940	0.49094985333
2.0	0.0	-1.55385466183	0.69833551958	-1.55385461770	0.69833551958
0.1	0.5	1.50290153802	0.54373594720	1.50290154558	0.543735194382
2.0	0.5	-1.86160632769	0.57094205000	-1.86160631992	0.570944204838
0.1	1.0	1.78958135566	0.58457144777	1.78958135810	0.58457144495
2.0	1.0	-2.12871045575	0.46338285937	-2.12871045195	0.46338286024

3.6.1 The Velocity Profiles

- Figure 3.2 displays the influence of Casson parameter δ when $R = 0.1$ and $R = 2$ on $f'(\eta)$. As $R < 1$, rise in the value of δ steeps the velocity profile, on contrary by fixing $R = 2$ the increase in δ deplete the $f'(\eta)$.

- Figure 3.3 depicts that the momentum BL thickness lessen when magnetic parameter M is increased with $R > 1$. This behaviour is due to the Lorentz force produced by magnetic field.

- In Figure 3.4 variation in the results of wedge angle β against the velocity profile $f'(\eta)$ is displayed. For $R > 1$ the increase in β results a increase in velocity profile, but for $R = 0.5$ it shows contrary behaviour.

- Figure 3.5 shows the behaviour of velocity ratio parameter on $f'(\eta)$. By increasing the values of R velocity profile also increases.

- Figure 3.6 - 3.7 display the impact of Nr and Pr. By increasing values of Prandtl number $f'(\eta)$ decreases and for reducing values of Nr thickness of velocity BL decreases.

- Figure 3.8 is presented to depict the impact of convective parameter Bi means the proportion of internal conductive resistance within the body to the outward convective resistance measured at the surface of the body. It is noted that an increase in internal conductive resistance instead of external convective resistance results the improvement in temperature which in return increase the velocity profile $f'(\eta)$.

- Figure 3.9 represent the significant results of Eckert number as Ec increases velocity profile goes downward when we choose $R < 1$.

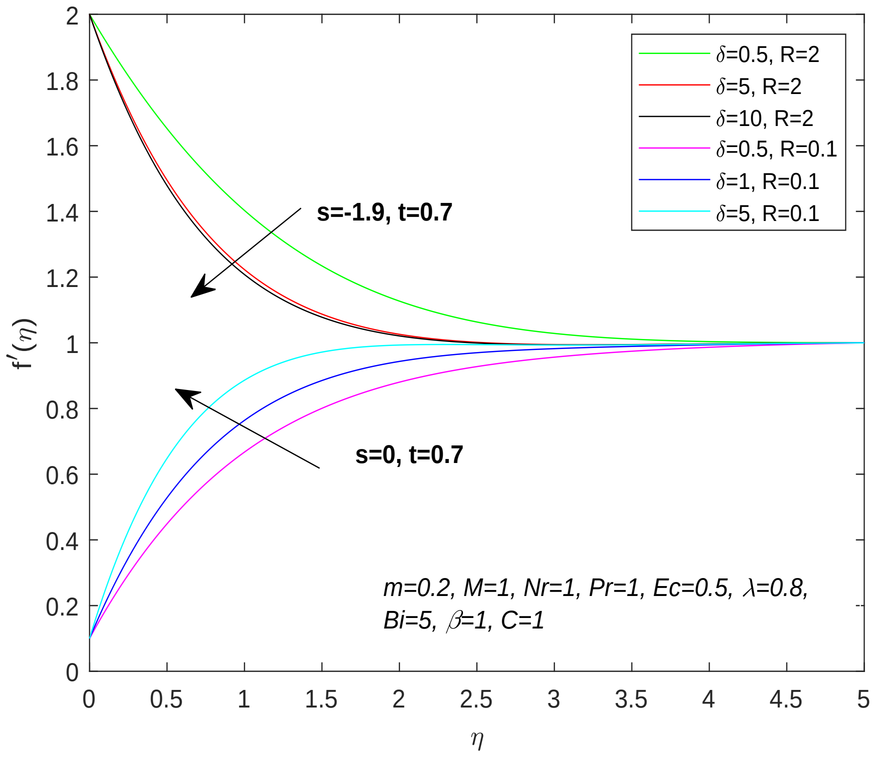

FIGURE 3.2: δ varies in $f'(\eta)$

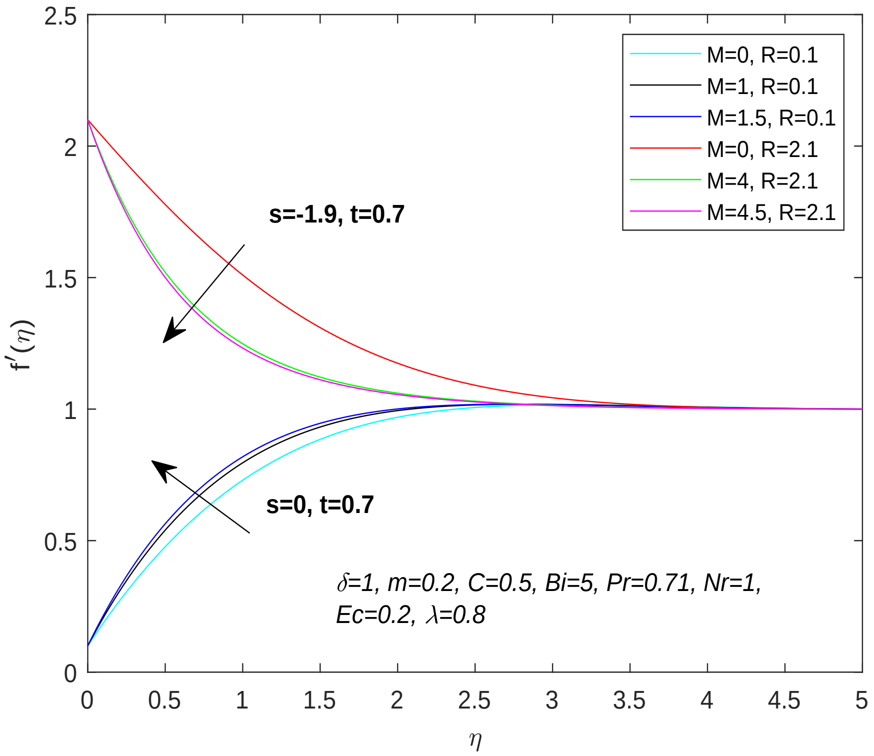

Figure 3.3: M varies in $f'(\eta)$

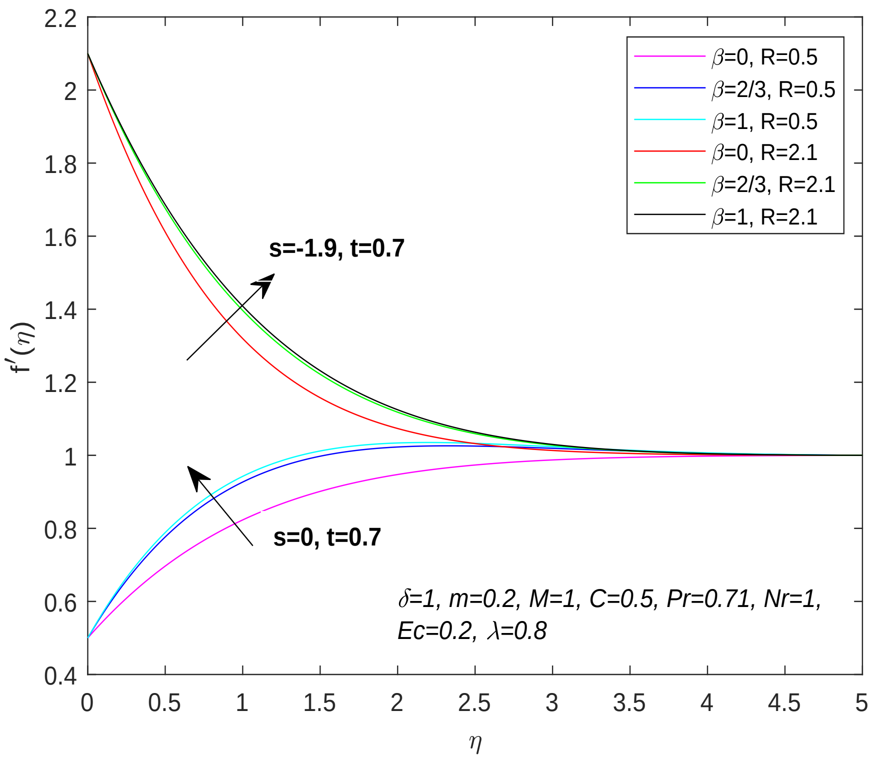

Figure 3.4: β varies in $f'(\eta)$

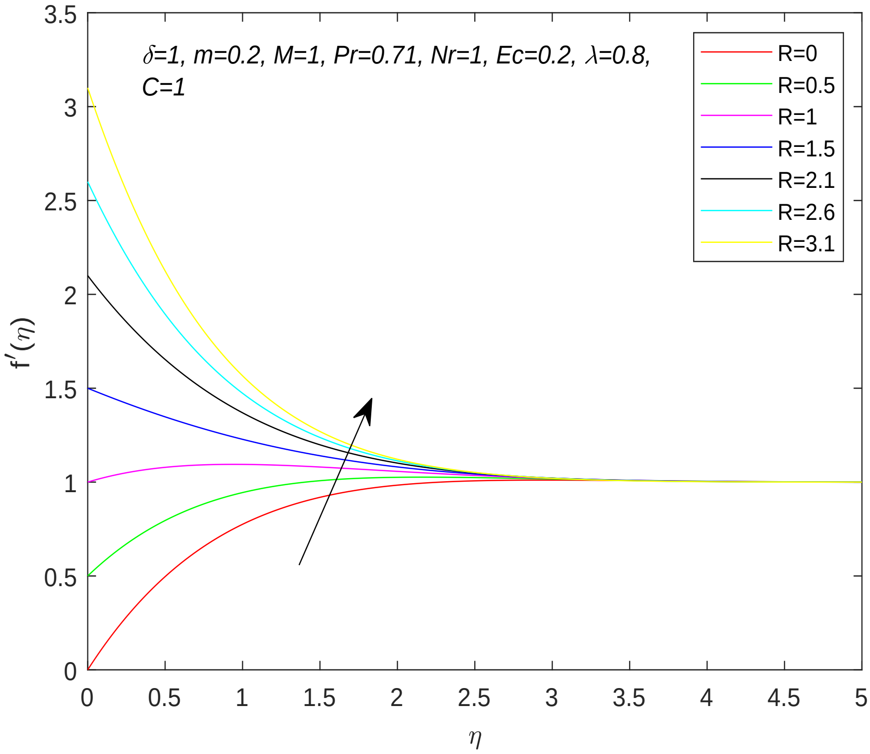

FIGURE 3.5: $f'(\eta)$ for several values of R

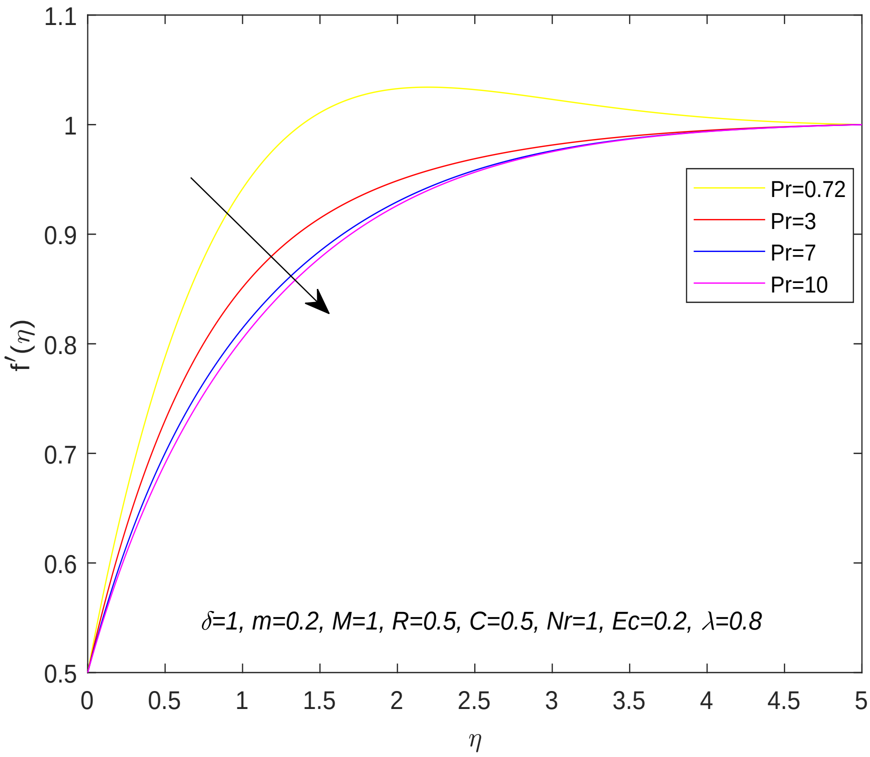

FIGURE 3.6: $f'(\eta)$ for multiple values of Pr

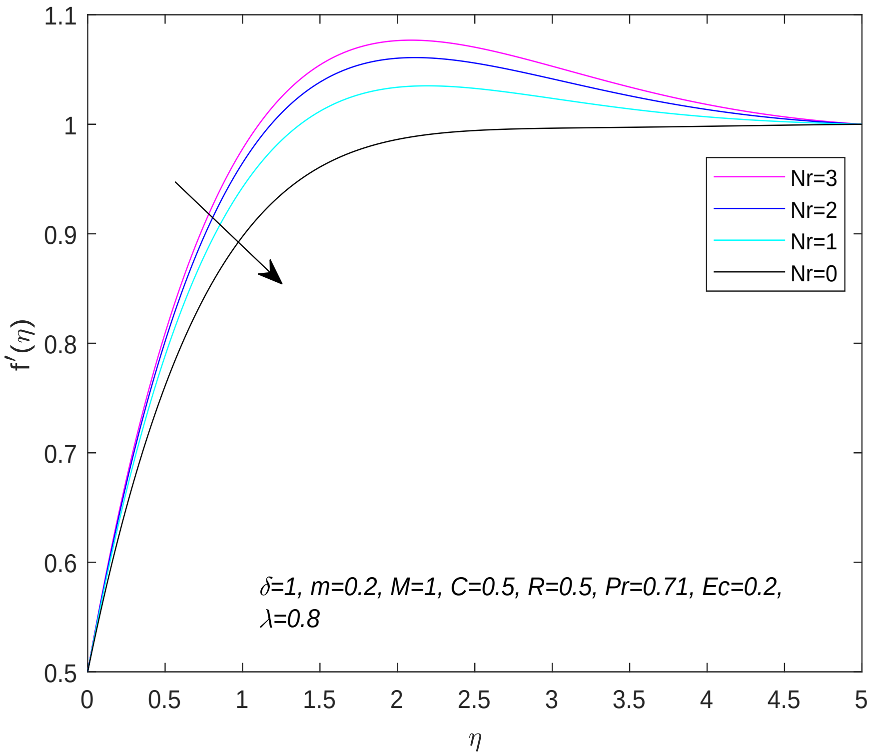

FIGURE 3.7: $f'(\eta)$ for multiple values of Nr

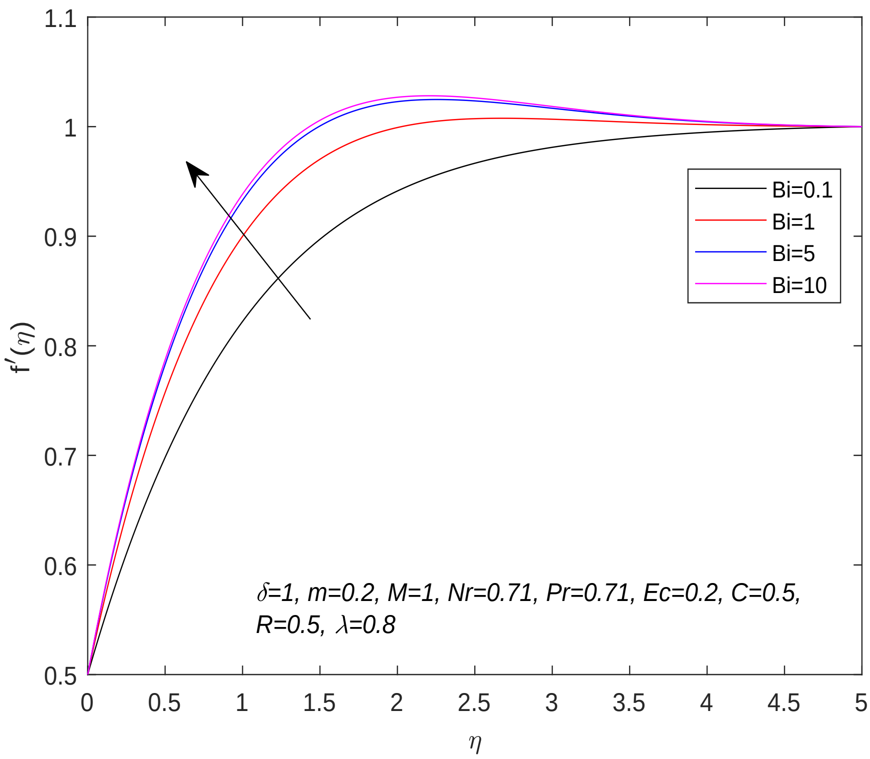

FIGURE 3.8: $f'(\eta)$ for various values of B_i

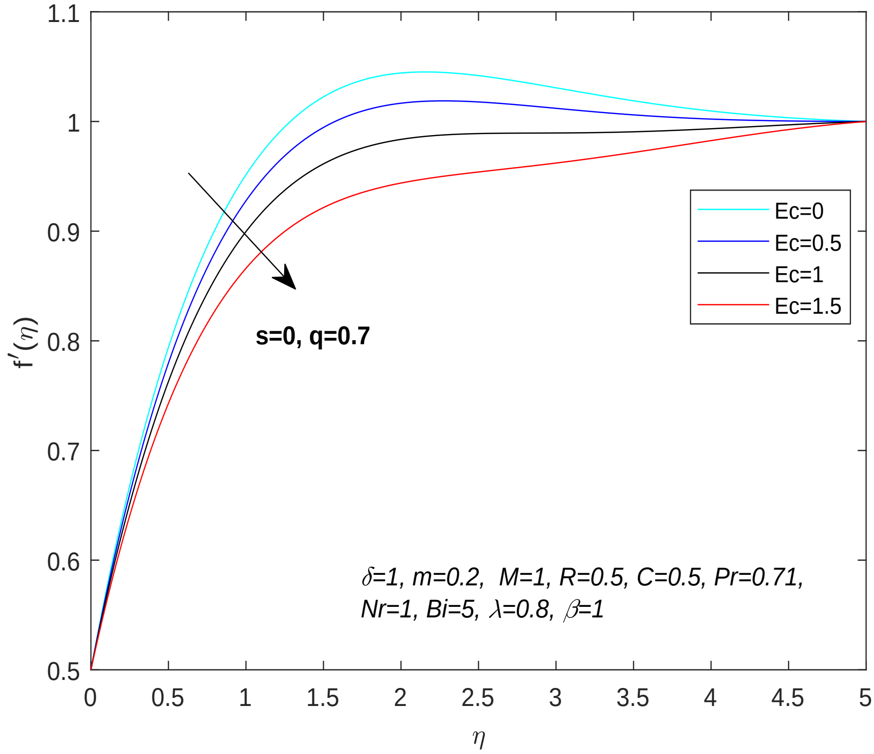

FIGURE 3.9: $f'(\eta)$ for various values of Ec

3.6.2 The Temperature Profile

- Figure 3.10 exhibits the effect of Casson parameter δ when $R = 0.5$ and $R = 2.1$ on $\theta(\eta)$. When $R < 1$, the increase in the value of δ steeps the temperature profile, but on contrary when $R = 2.1$, the increase in δ reduce the thickness of temperature BL $\theta(\eta)$.

- In Figure 3.11 the impact of magnetic parameter on temperature boundary layer $\theta(\eta)$ is displayed. This graph check that when $R > 1$, the increase in M leads temperature profile to go upward but when $R = 0.1$ the behaviour is opposite.

- Figure 3.12 is exhibited to discuss the effect of wedge inclination β on temperature. For both cases $R = \mathbb{R} - \{1\}$, increase in wedge angle decreases the temperature profile $\theta(\eta)$.

- Figure 3.13 shows the effect of Nr on $\theta(\eta)$. This figure shows that by decreasing values of Nr temperature profile also diminish.

- Figure 3.14 displays that by rising values of R velocity ratio parameter, temperature profile $\theta(\eta)$ decreased.

- Figure 3.15-3.16 display the influence of Ec and Pr. By increasing values of Eckert number, the temperature profile $\theta(\eta)$ decreases and with increase in the values of Pr, temperature profile lessens.

- Figure 3.17 shows the impact of Biot umber B_i means the proportion of internal conductive resistance within the body to the outward convective resistance measured at the surface of the body. By rising values of conductive heat transfer resistance the temperature profile $\theta(\eta)$ also increases.

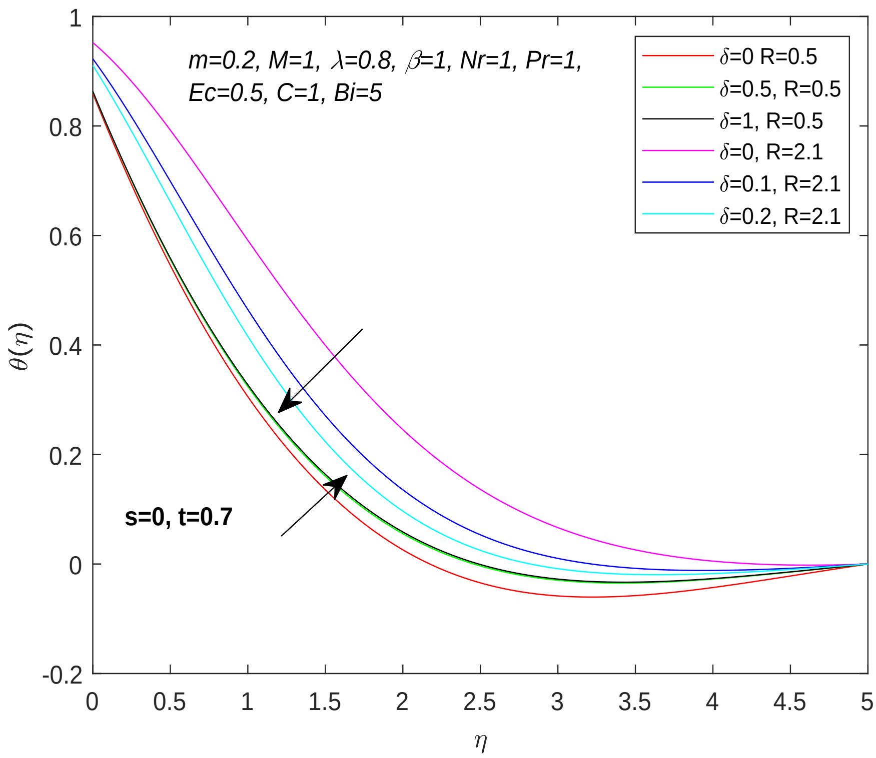

FIGURE 3.10: Variation in $\theta(\eta)$ for different values of δ

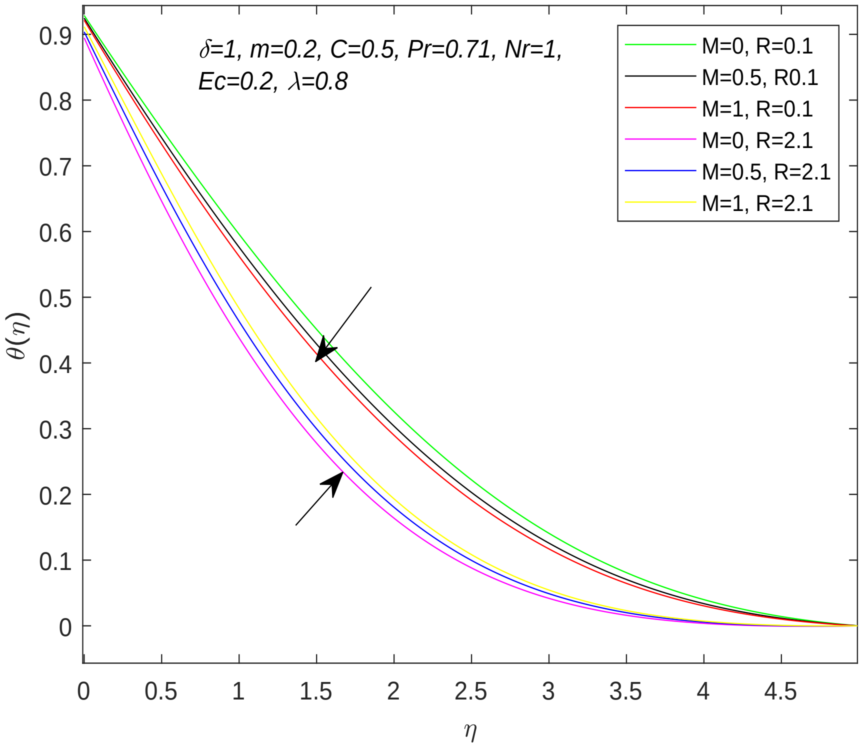

FIGURE 3.11: Variation in $\theta(\eta)$ for multiple values of M

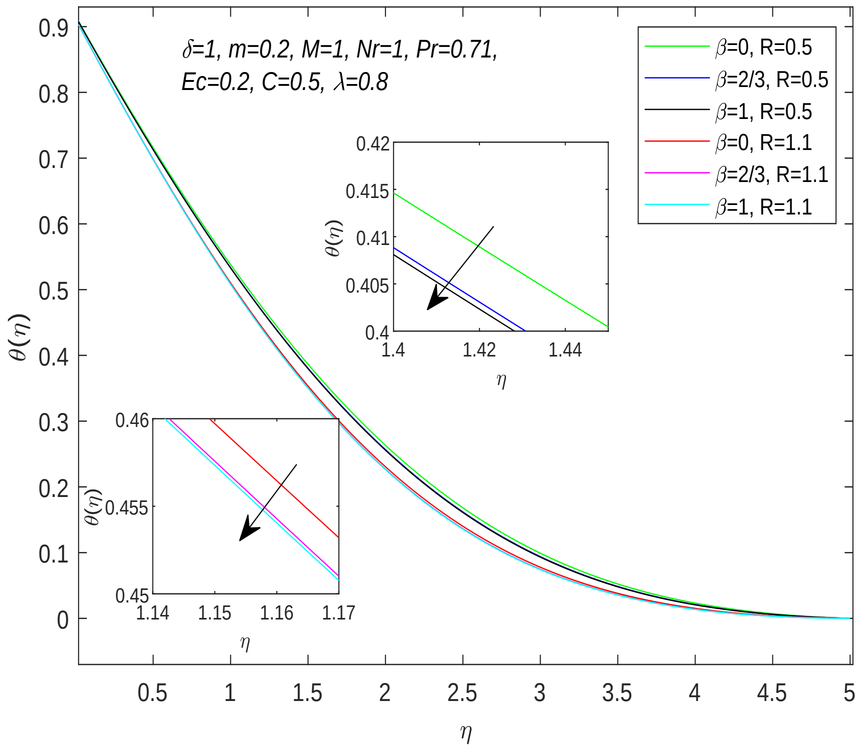

FIGURE 3.12: Variation in $\theta(\eta)$ for several values of β

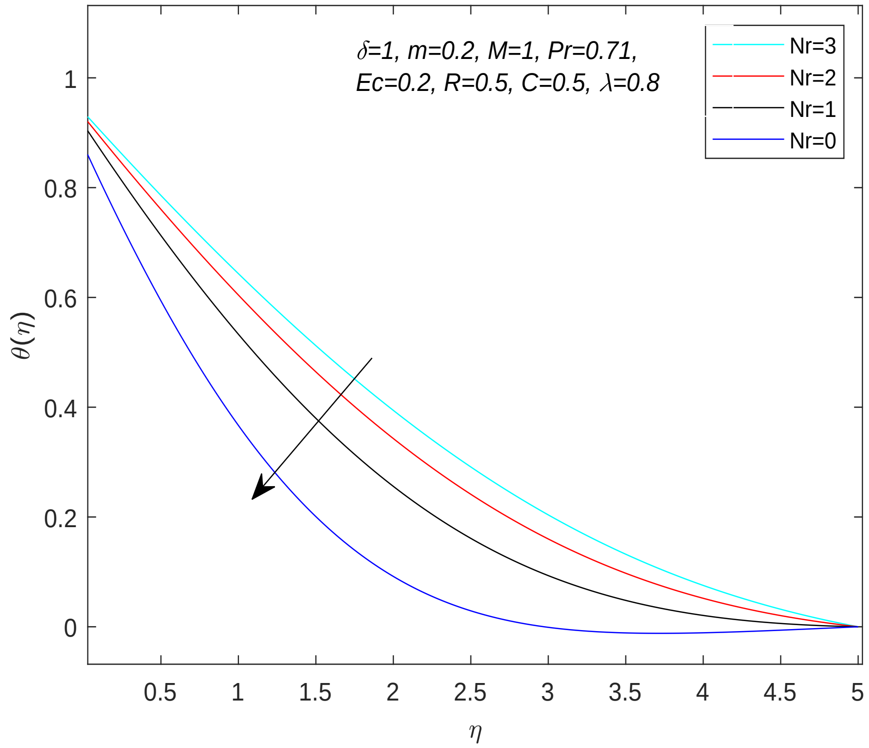

FIGURE 3.13: $\theta(\eta)$ for various values of Nr

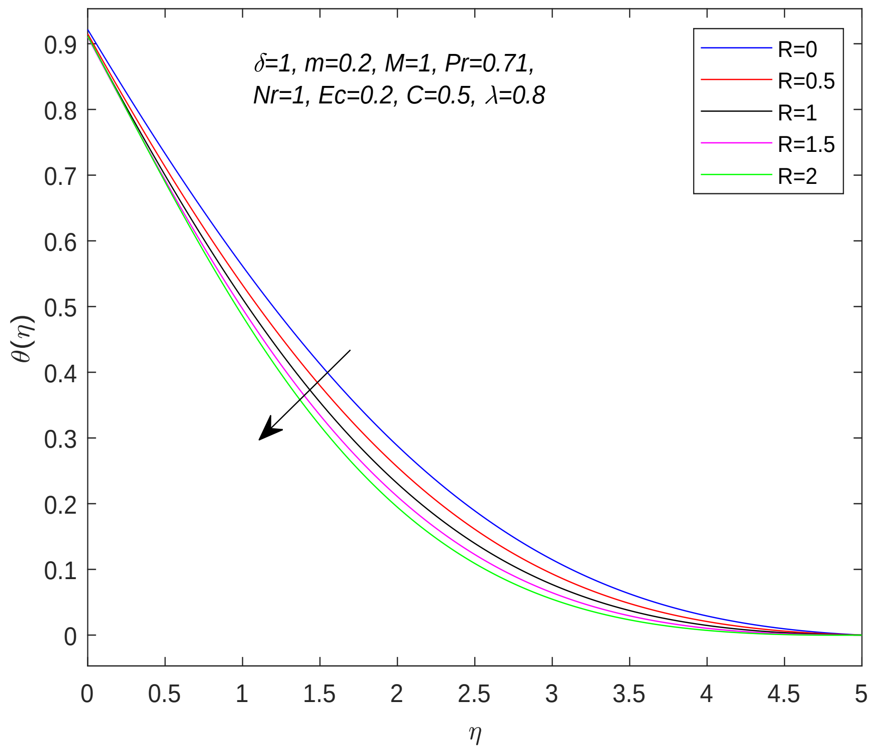

FIGURE 3.14: Variation in $\theta(\eta)$ for multiple values of R

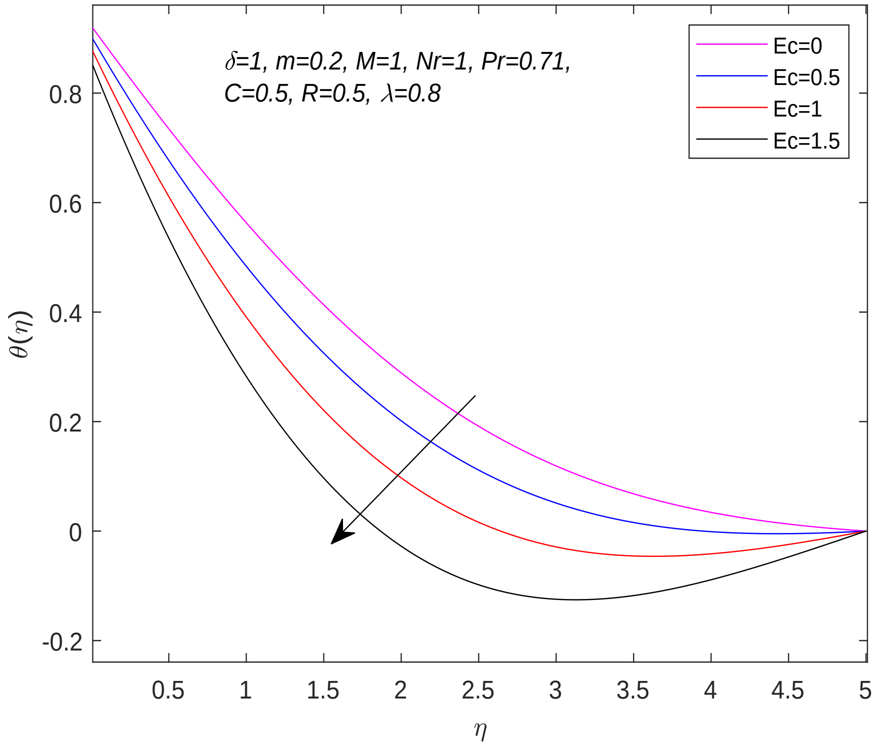

FIGURE 3.15: Variation in $\theta(\eta)$ for various values of Ec

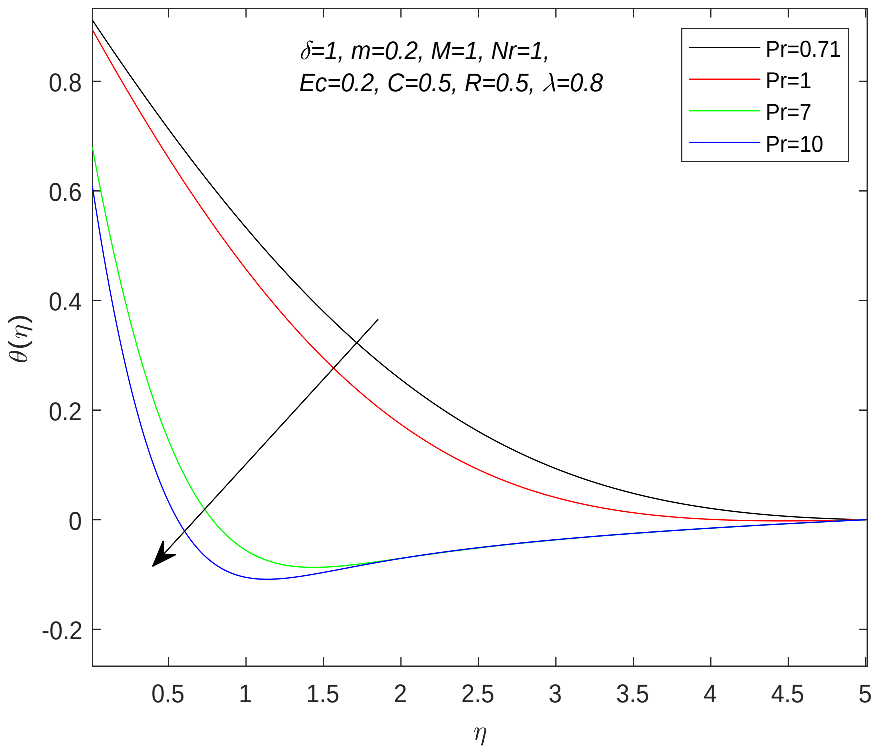

FIGURE 3.16: Temperature profile for various values of Pr

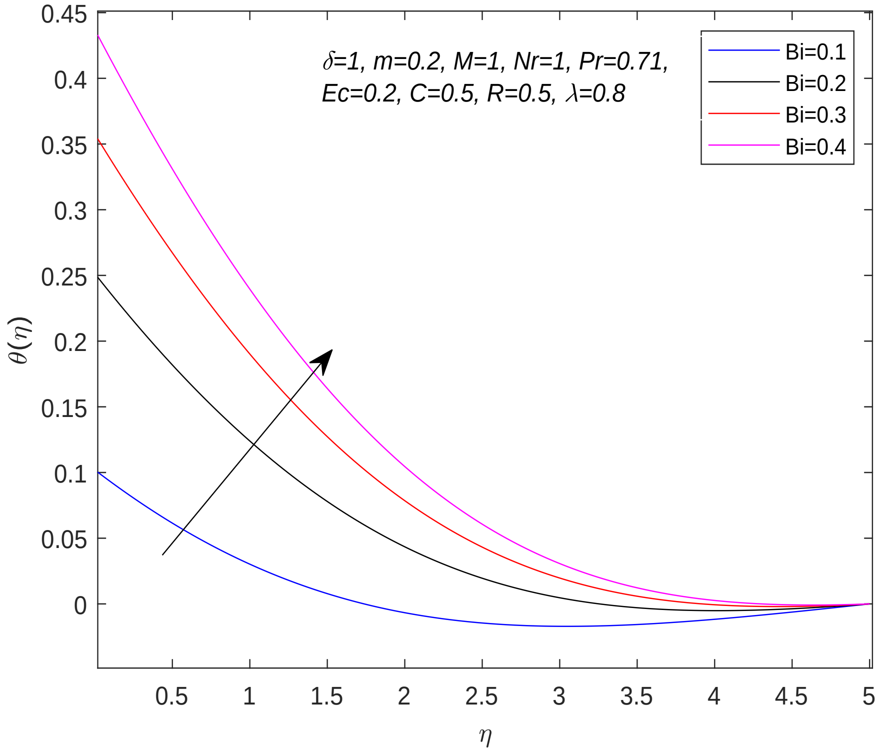

FIGURE 3.17: Variation in $\theta(\eta)$ for various values of B_i

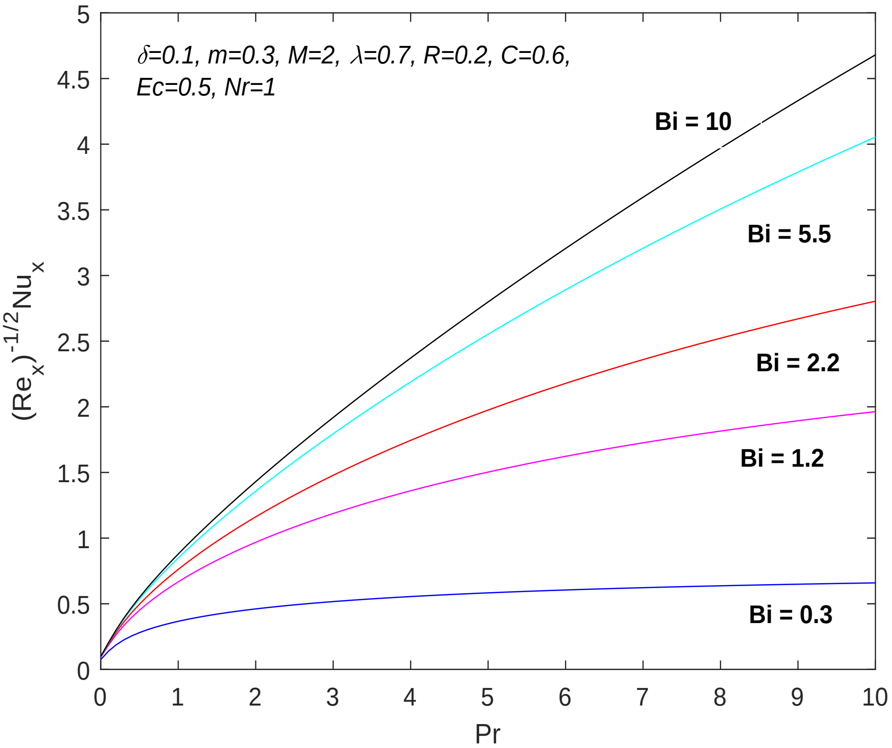

FIGURE 3.18: Nusselt number for different values of B_i

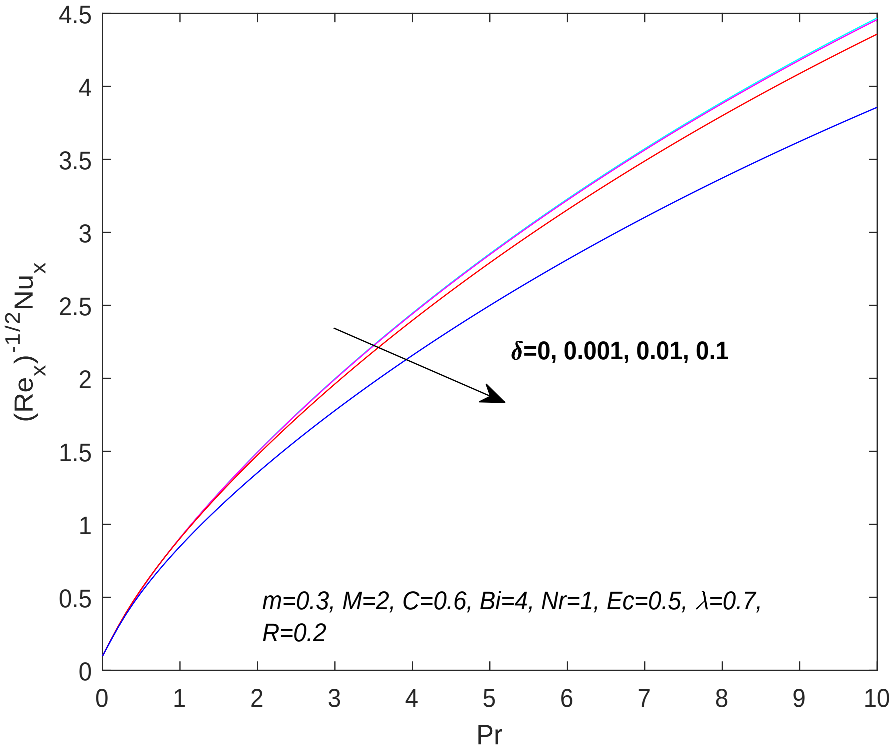

FIGURE 3.19: Nusselt number for various values of δ

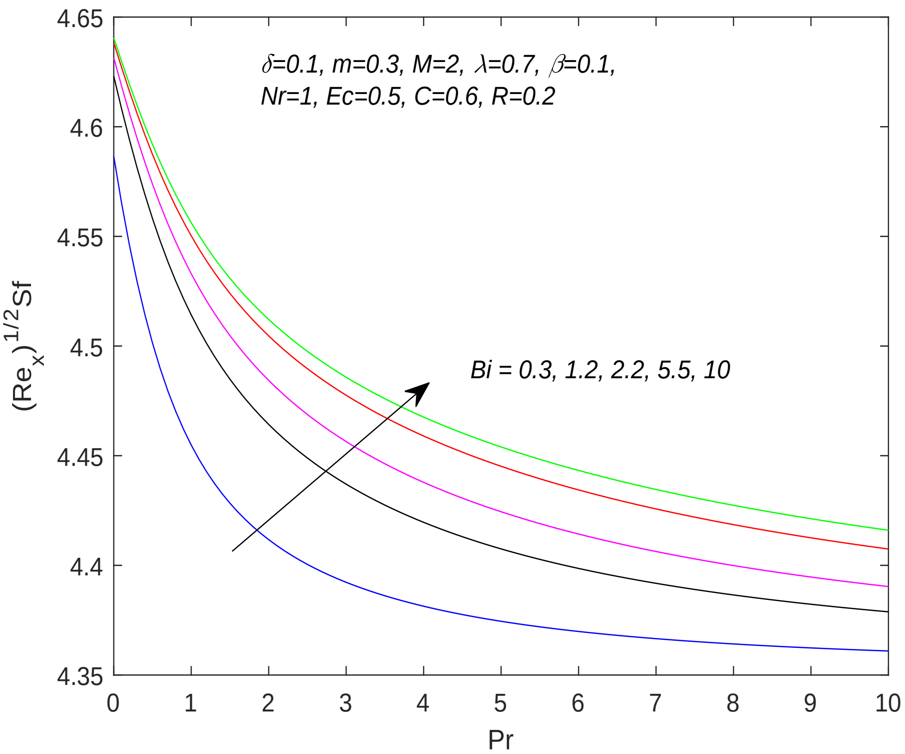

FIGURE 3.20: Surface drag force for varied values of B_i

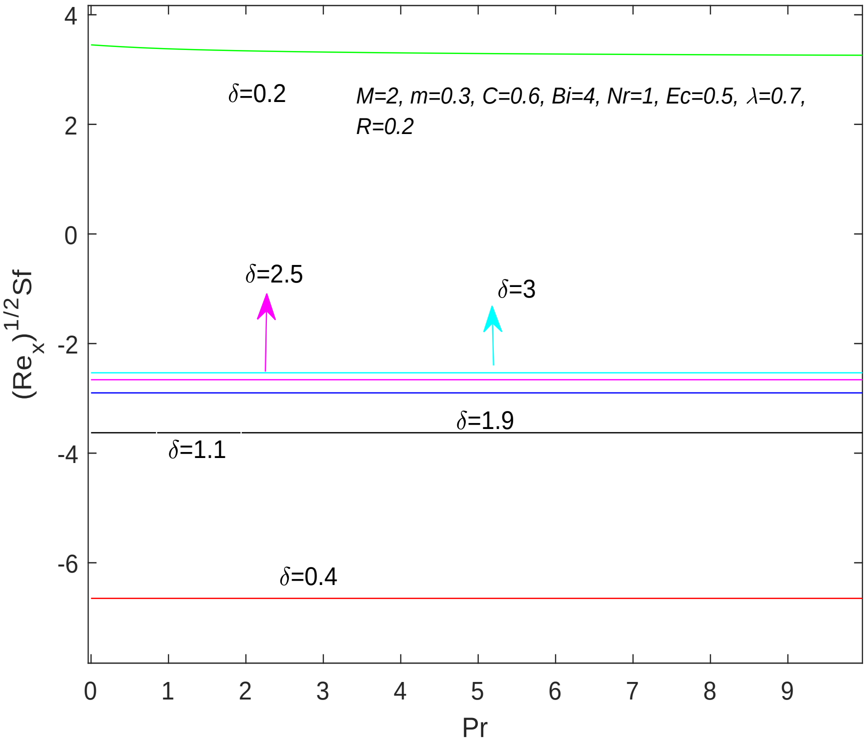

FIGURE 3.21: Surface drag force for varied values of δ

3.6.3 Nusselt Number and Surface Drag Force Coefficient

- Figures 3.18 - 3.20 show the impact of Biot number on Nusselt number $(Re_x)^{\frac{-1}{2}} Nu_x$ and skin friction $(Re_x)^{\frac{1}{2}} C_f$. The increasing values of Biot number, accelerate the drag force and Nusselt number.

- Figures 3.19 - 3.21 depict the impact of casson parameter on Nusselt number $(Re_x)^{\frac{-1}{2}} Nu_x$ and skin friction $(Re_x)^{\frac{1}{2}} C_f$. The increasing value of Casson Parameter results an increase in drag force and a decrease in Nusselt number.

Chapter 4

Flow Problem of Casson Fluid over a Stretching Porous Wedge with Viscous Dissipation

4.1 Introduction

This chapter extends the work of [27] by considering the effects of porosity paramters and viscous dissipation. The extended momentum and energy equations are in the form of PDEs. This system of PDEs is transformed into set of ODEs. The BVPs are numerically solved using the shooting method. The results of the procedure are then validated using inbuilt command bvp4c of the MATLAB. The temperature $\theta(\eta)$ and velocity $f'(\eta)$ profiles are then described through graphs and tables.

4.2 Mathematical Modeling

Extended PDEs are as follows:

$$\frac{\partial u}{\partial x} + \frac{\partial v}{\partial y} = 0, \tag{4.1}$$

$$u\frac{\partial u}{\partial x}+v\frac{\partial u}{\partial y}=U\frac{dU}{dx}+\nu\Big(1+\frac{1}{\delta}\Big)\frac{\partial^2 u}{\partial y^2}+g\beta_o(T-T_\infty)Sin\frac{\Omega}{2}-\frac{\sigma B^2}{\rho}(u-U)-$$
$$\frac{\nu\Phi u}{k}-\frac{C_b\Phi u^2}{\sqrt{k}}, \tag{4.2}$$
$$\rho c_p\Big(u\frac{\partial T}{\partial x}+v\frac{\partial T}{\partial y}\Big)=-u\Big(\rho U\frac{dU}{dx}+\sigma B^2U\Big)+\alpha\frac{\partial^2 T}{\partial y^2}-\frac{\partial q_r}{\partial y}+\sigma B^2u^2+\frac{\mu}{\rho c_p}\Big(\frac{\partial u}{\partial y}\Big)^2. \tag{4.3}$$

The suitable BCs of the given problem are:

$$u(x,0)=RU, \tag{4.4}$$
$$v(x,0)=v_w=-(vU_o)^{\frac{1}{2}}C\Big(\frac{m+1}{2}\Big)x^{\frac{m+1}{2}}, \tag{4.5}$$
$$\frac{\partial T(x,0)}{\partial y}=\frac{h}{k}(T-T_f), \tag{4.6}$$
$$u(x,\infty_n)\ \rightarrow\ U_ox^m,\quad T(x,\infty_n)\ \rightarrow\ T_{\infty_n}. \tag{4.7}$$

Following transformations are used to change the PDEs into non-dimensional form:

$$\begin{aligned}
&=\sqrt{U\nu x}f,\\
u&=\frac{\partial\psi}{\partial y},\\
v&=-\frac{\partial\psi}{\partial x},\\
\eta&=\sqrt{\frac{U_o}{\nu}}x^{\frac{m-1}{2}}y,\\
\theta(\eta)&=\frac{T-T_\infty}{T_f-T_\infty}.
\end{aligned}$$

Conversion of continuity equation is already discussed in previous chapter. Here, conversion of equations (4.2) and (4.3) is discussed. Now the extended momentum equation is converted into non-dimensional form:

$$u\frac{\partial u}{\partial x}+v\frac{\partial u}{\partial y}=mU_o^2x^{2m-1}f'^2+U_o^2\frac{m-1}{2}x^{2m-1}\eta f'f''-U_o^2x^{2m-1}\frac{m+1}{2}ff''-$$
$$U_o^2x^{2m-1}\frac{m-1}{2}\eta f'f'',$$

$$U\frac{dU}{dx}+\nu\Big(1+\frac{1}{\delta}\Big)\frac{\partial^2 u}{\partial y^2}+g\beta_o(T-T_\infty)Sin\frac{\Omega}{2}-\frac{\sigma B^2}{\rho}(u-U)-\frac{\nu\Phi u}{k}-\frac{C_b\Phi u^2}{\sqrt{k}}=$$
$$mU_o^2x^{2m-1}+U_o^2x^{2m-1}\Big(1+\frac{1}{\delta}\Big)f'''+g\beta_o\theta(T_f-T_\infty)Sin\frac{\Omega}{2}-x^{2m-1}MU_o^2(f'-1)-$$
$$\frac{\nu\Phi U_o x^m f'}{k}-\frac{C_b\Phi U_o^2x^{2m}f'^2}{\sqrt{k}}.$$

Equating above equations:

$$\Big[mf'^2-\frac{m+1}{2}ff''\Big]=\Big[m+\Big(1+\frac{1}{\delta}\Big)f'''+\lambda Sin\frac{\Omega}{2}\theta-M(f'-1)-\frac{\nu\Phi f'}{kU_ox^{m-1}}-$$
$$\frac{C_b\Phi xf'^2}{\sqrt{k}}\Big],$$
$$f'''\Big(1+\frac{1}{\delta}\Big)+\Big(\frac{m+1}{2}\Big)ff''+(1-f'^2)m-M(f'-1)+\lambda Sin\frac{\Omega}{2}\theta-\frac{\nu\Phi f'}{kU_ox^{m-1}}-$$
$$\frac{C_b\Phi xf'^2}{\sqrt{k}}=0,$$
$$f'''=\Big(1+\frac{1}{\delta}\Big)\Big[-\frac{m+1}{2}ff''-m+mf'^2+Mf'-M-\lambda Sin\frac{\Omega}{2}\theta+Da^{-1}f'+$$
$$\alpha_1f'^2\Big],$$
$$f'''=\Big(1+\frac{1}{\delta}\Big)\Big[-\frac{m+1}{2}ff''-(m+M)+(m+\alpha_1)f'^2+(M+(Da)^{-1})f'-$$
$$\lambda Sin\frac{\Omega}{2}\theta\Big]. \tag{4.8}$$

These parameters $(Da)^{-1}=\dfrac{\nu\Phi}{kU_ox^{m-1}}$ and $\alpha_1=\dfrac{C_b\Phi x}{\sqrt{k}}$ are used in above equations. Dimensionless form of energy equation is:

$$\rho c_p\Big(u\frac{\partial T}{\partial x}+v\frac{\partial T}{\partial y}\Big)=-u\Big(\rho U\frac{dU}{dx}+\sigma B^2U\Big)+\alpha\frac{\partial^2T}{\partial y^2}-\frac{\partial q_r}{\partial y}+\sigma B^2u^2+\frac{\mu}{\rho c_p}\Big(\frac{\partial u}{\partial y}\Big)^2,$$
$$\rho c_p\Big(u\frac{\partial T}{\partial x}+v\frac{\partial T}{\partial y}\Big)=\rho c_p\Big[-U_ox^{m-1}\Big(\frac{m+1}{2}\Big)(T_f-T_\infty)f\theta'\Big],$$
$$-u\Big(\rho U\frac{dU}{dx}+\sigma B^2U\Big)+\alpha\frac{\partial^2T}{\partial y^2}-\frac{\partial q_r}{\partial y}+\sigma B^2u^2+\frac{\mu}{\rho c_p}\Big(\frac{\partial u}{\partial y}\Big)^2=$$
$$-\rho mU_o^3x^{3m-1}f'-\sigma B_o^2U_o^2x^{3m-1}f'+\alpha(T_f-T_\infty)\frac{U_o}{\nu}x^{m-1}\theta''+$$
$$\frac{16\sigma_0T_\infty^3}{3k^*}(T_f-T_\infty)\frac{U_o}{\nu}\theta''x^{m-1}+\sigma B_o^2x^{3m-1}U_o^2(f')^2+\frac{\mu}{\rho c_p}(\frac{\partial u}{\partial y})^2.$$

Now the L.H.S equals to R.H.S of energy equation is given below:

$$\rho c_p\Big[-U_o x^{m-1}\Big(\frac{m+1}{2}\Big)(T_f-T_\infty)f\theta'\Big]=-\rho m U_o^3 x^{3m-1}f'-\sigma B_o^2U_o^2x^{3m-1}f'+$$
$$\alpha\big(T_f-T_\infty\big)\frac{U_o}{\nu}x^{m-1}\theta''+\frac{16\sigma_0T_\infty^3}{3k^*}\big(T_f-T_\infty\big)\frac{U_o}{\nu}\theta''x^{m-1}+\sigma B_o^2x^{3m-1}U_o^2\big(f'\big)^2+$$
$$\frac{\mu}{\rho c_p}\big(\frac{\partial u}{\partial y}\big)^2,$$
$$\Big[-\Big(\frac{m+1}{2}\Big)f\theta'\Big]=-\frac{mU_o^2x^{2m}f'}{c_p(T_f-T_\infty)}-\frac{\sigma B_o^2U_ox^{2mf'}}{\rho c_p(T_f-T_\infty)}+\frac{\alpha\theta''}{\rho c_p\nu}+\frac{16T_\infty^3\sigma_0\theta''}{3k^*\rho c_p\nu}+$$
$$\frac{\sigma B_o^2U_ox^{2m}f'^2}{\rho c_p(T_f-T_\infty)}+\frac{\mu}{\rho^2c_p^2U_ox^{m-1}}\Big(\frac{U_o^3x^{3m-1}f''^2}{\nu(T_f-T_\infty)}\Big),$$
$$\Big(\frac{m+1}{2}\Big)f\theta'-\frac{mU^2f'}{c_p(T_f-T_\infty)}-\frac{\sigma B_o^2U_ox^{2mf'}}{\rho c_p(T_f-T_\infty)}+\frac{\alpha}{\mu c_p}(1+Nr)\theta''+\frac{\sigma B_o^2U_ox^{2m}f'^2}{\rho c_p(T_f-T_\infty)}+$$
$$\frac{\mu U^2f''^2}{\rho^2c_p^2\nu(T_f-T_\infty)}=0,$$

Multiply above equation with $\dfrac{\mu c_p}{\alpha}$ and we get:

$$(1+Nr)\theta''+\frac{\mu c_p}{\alpha}\Big(\frac{m+1}{2}\Big)f\theta'-\frac{\mu mU^2f'}{\alpha(T_f-T_\infty)}-\frac{\sigma B_o^2U_ox^{2m}\mu f'}{\rho\alpha(T_f-T_\infty)}+$$
$$\frac{\sigma B_o^2U_ox^{2m}\mu f'^2}{\rho\alpha(T_f-T_\infty)}+\frac{\mu^2U^2f''^2}{\rho^2c_p\alpha\nu(T_f-T_\infty)}=0,$$
$$(1+Nr)\theta''+Pr\Big(\frac{m+1}{2}\Big)f\theta'-mEcPrf'-MEcPrf'+MEcPrf'^2+$$
$$\frac{\mu^2Ecf''^2}{\rho^2\alpha\nu}=0,$$
$$(1+Nr)\theta''+Pr\Big(\frac{m+1}{2}\Big)f\theta'-mEcPrf'-MEcPrf'+MEcPrf'^2+$$
$$PrEcf''^2=0,$$
$$\theta''=\frac{-1}{(1+Nr)}\Big[Pr\Big(\frac{m+1}{2}\Big)f\theta'-mEcPrf'-MEcPrf'+MEcPrf'^2+$$
$$PrEcf''^2\Big]. \tag{4.9}$$

Final form of dimensionless momentum and energy equation are given below:

$$f'''=\Big(1+\frac{1}{\delta}\Big)\Big[-\frac{m+1}{2}ff''-(m+M)+(m+\alpha_1)f'^2+(M+(Da)^{-1})f'-$$
$$\lambda Sin\frac{\Omega}{2}\theta\Big], \tag{4.10}$$

$$\theta'' = \frac{-1}{(1+Nr)}\Big[Pr\Big(\frac{m+1}{2}\Big)f\theta' - mEcPrf' - MEcPrf' + MEcPrf'^2 + PrEcf''^2\Big]. \tag{4.11}$$

Along with similiar dimensionless boundary conditions of previous chapter are also used here.

$$\left.\begin{aligned} \theta'(0) &= -B_i + B_i\,\theta(0),\ \theta(\infty_n) \ = \ 0. \\ f(0) \ &= \ C,\ f'(0) \ = \ R,\ f'(\infty_n) \ = \ 1. \end{aligned}\right\} \tag{4.12}$$

4.3 Shooting Method

The shooting method is applied on BVP given by (4.10) and (4.11) along with boundary conditions (4.12). Using the following notation the BVP is converted into an initial value problem.

$$\begin{aligned} f &= y_1, \\ f' &= y_1' = y_2, \\ f'' &= y_2' = y_3, \\ f''' &= y_3', \\ \theta &= y_4, \\ \theta' &= y_4' = y_5, \\ \theta'' &= y_5'. \end{aligned}$$

Using the above notations (4.10) and (4.11) are transformed into three five first order differential equations

$$y_1' = y_2 \ \ ; \qquad\qquad y_1(0) = C,$$

$$y_2' = y_3 \ \ ; \qquad\qquad y_2(0) = R, \quad y_2(\infty) = 1,$$

$$y_3' = \Big(1+\frac{1}{\delta}\Big)\Big[-\frac{m+1}{2}y_1y_3 - (m+M) + (m+\alpha_1)y_2^2 + (M+(Da)^{-1})y_2 - \lambda Sin\frac{\Omega}{2}y_4\Big], \qquad\qquad y_3(0) = s,$$

$$y_4' = y_5 \quad ; \qquad\qquad y_4(0) = q, \quad y_4(\infty) = 0,$$
$$y_5' = \frac{-1}{\big(1+Nr\big)}\Big[Pr\Big(\frac{m+1}{2}\Big)y_1y_5 - mEcPry_2 - MEcPry_2 + MEcPry_2^2 +$$
$$PrEcy_3^2\Big], \qquad\qquad y_5(0) = -Bi(1-q).$$

where s and q are the missing initial conditions. Now the above first order initial value problem is solved by applying RK-4 technique. The missing conditions are to be selected such as:

$$y_2(\infty_n, s, q) = 1, \quad y_4(\infty_n, s, q) = 0.$$

Denote

$$\phi_1(s,q) = y_2(\infty_n, s, q) - 1,$$
$$\phi_2(s,q) = y_4(\infty_n, s, q).$$

If $\phi_1(s,q) = 0$ and $\phi_2(s,q) = 0$ then we get our solution, if not we use Newton's Raphson method to refine the following iterative formula:

$$\begin{bmatrix} s \\ q \end{bmatrix}_{(n+1)} = \begin{bmatrix} s \\ q \end{bmatrix}_n - \begin{bmatrix} \dfrac{\partial y_2}{\partial s} & \dfrac{\partial y_2}{\partial q} \\ \dfrac{\partial y_4}{\partial s} & \dfrac{\partial y_4}{\partial q} \end{bmatrix}_n^{-1} \begin{bmatrix} \phi_1 \\ \phi_2 \end{bmatrix}_n . \qquad (4.13)$$

Following notations are used to calculate the new appeared derivatives:

$$\frac{\partial y_1}{\partial s} = y_6, \frac{\partial y_2}{\partial s} = y_7, \frac{\partial y_3}{\partial s} = y_8, \frac{\partial y_4}{\partial s} = y_9, \frac{\partial y_5}{\partial s} = y_{10}.$$
$$\frac{\partial y_1}{\partial q} = y_{11}, \frac{\partial y_2}{\partial q} = y_{12}, \frac{\partial y_3}{\partial q} = y_{13}, \frac{\partial y_4}{\partial q} = y_{14}, \frac{\partial y_5}{\partial q} = y_{15}.$$

We get the following equations by differentiating above IVP with respect to s and q

$$y_6' = y_7 \quad ; \qquad\qquad y_6(0) = 0,$$
$$y_7' = y_8 \quad ; \qquad\qquad y_7(0) = 0, \quad y_7(\infty) = 0,$$

$$y_8' = \frac{1}{\left(1+\frac{1}{\delta}\right)}\Big[-\frac{m+1}{2}(y_6y_3 + y_1y_8) + 2(m+\alpha_1)y_2y_7 + (M+(Da)^{-1})y_7 -$$

$$\lambda Sin\frac{\Omega}{2}y_9\Big], \qquad y_8(0) = 1,$$

$$y_9' = y_{10} \; ; \qquad y_9(0) = 0, \quad y_9(\infty) = 0,$$

$$y_{10}' = \frac{-1}{(1+Nr)}\Big[Pr\Big(\frac{m+1}{2}\Big)(y_6y_5 + y_1y_{10}) - mEcPry_7 - MEcPry_7 +$$

$$2MEcPry_2y_7 + 2PrEcy_3y_8\Big], \qquad y_{10}(0) = 0.$$

$$y_{11}' = y_{12} \; ; \qquad y_{11}(0) = 0,$$

$$y_{12}' = y_{13} \; ; \qquad y_{12}(0) = 0, \quad y_{12}(\infty) = 0,$$

$$y_{13}' = \frac{1}{\left(1+\frac{1}{\delta}\right)}\Big[-\frac{m+1}{2}(y_{11}y_3 + y_1y_{13}) + 2(m+\alpha_1)y_2y_{12} + (M+Da^{-1})y_{12} -$$

$$\lambda Sin\frac{\Omega}{2}y_{14}\Big], \qquad y_{13}(0) = 0,$$

$$y_{14}' = y_{15} \; ; \qquad y_{14}(0) = 1, \quad y_{14}(\infty) = 0,$$

$$y_{15}' = \frac{1}{\left(1+Nr\right)}\Big[-Pr\Big(\frac{m+1}{2}\Big)\big(y_{11}y_5 + y_1y_{15}\big) + mEcPry_{12} +$$

$$MEcPry_{12} - 2MEcPry_2y_{12}\Big], \qquad y_{15}(0) = B_i.$$

Following stopping criteria is used for Newton's method:

$$max(\mid \phi_1(\eta_\infty, s_n, q_n) \mid, \mid \phi_2(\eta_\infty, s_n, q_n) \mid) < \epsilon.$$

Here, $\epsilon = 10^{-8}$.

4.4 Results and Discussions

Table 4.1 depicts the value of skin fricktion and Nusselt number for various values of velocity ratio parameter R and wedge angle β. On both cases when $R < 1$ or $R > 1$, by increasing values of wedge angle parameter β, surface drag force coefficient $f''(0)$ increases. It is also observed that with the increase of β the temperature gradient coefficient of Nusselt number $|\theta'(0)|$ also decreases. Results obtained by shooting method are also validated by bvp4c. Here, the values of diferent parameters are fixed such as $\delta = 1$, $m = 0.1$, $\lambda = 0.8$, $B_i = 5$, $M = 0$, $Nr = 1$, $Pr = 1$, $Ec = 0.5$ and $C = 1$, $(Da)^{-1} = 0.01$ and $\alpha_1 = 0.01$

TABLE 4.1: Results of $(Re_x)^{\frac{1}{2}}C_f$ and $(Re_x)^{\frac{-1}{2}}Nu_x$ for values of β.

		Shooting		*bvp4c*	
R	β	C_f	Nu_x	C_f	Nu_x
0.3	0.0	1.69658760891	0.63337168742	1.69658760047	0.63337154600
2.0	0.0	-2.89008774386	0.45899909881	-2.89008775215	0.45899909775
0.3	0.7	2.07949724747	0.62651534840	2.07949724751	0.62651534840
2.0	0.7	-2.50129930834	0.45694769615	-2.50129931309	0.45694769229
0.3	1	2.13879844844	0.62521388870	2.13879844837	0.62521389153
2.0	1	-2.44050791207	0.45640487833	-2.44050791544	0.45640487686

Table 4.2 presents the values of drag force and Nusselt number as for multiple values of velocity ratio parameter R and momentum boundary layer M. When $R < 1$, by increasing values of magnetic parameter M, surface drag force coefficient $f''(0)$ also the values of temperature gradient coefficient of Nusselt number $|\theta'(0)|$ increases. When $R > 1$, by increasing values of magnetic parameter M, skin friction coefficient $f''(0)$ and the values of $|\theta'(0)|$ decreases. Results achieved by shooting technique are also satisfied by bvp4c.

TABLE 4.2: Results of $(Re_x)^{\frac{1}{2}}C_f$ and $(Re_x)^{\frac{-1}{2}}Nu_x$ for values of M.

		Shooting		*bvp4c*	
R	M	C_f	Nu_x	C_f	Nu_x
0.3	0.0	1.20318792005	0.54890507691	1.20318792186	0.49094985376
0.3	1.0	1.76577658883	0.63233066638	1.76577658484	0.63233066766
0.3	1.5	1.98524900184	0.66398690612	1.98524900046	0.66398690879
2.0	0.0	-2.19942925344	0.73146211947	-2.19942925346	0.73146211939
2.0	4.0	-4.17193636185	-0.10738670687	-4.17193636668	-0.10738670215
2.0	4.5	-4.35643483323	-0.18263653574	-4.35643483570	-0.18263653376

4.4.1 The Velocity Profiles

- Figure 4.1 displays how the Casson parameter δ affects $f'(\eta)$ when $R = \mathbb{R} - \{1\}$. As $R < 1$, increase in the value of δ steeps the velocity profile $f'(\eta)$, on contrary by fixing $R = 2$, the increase in δ deplete the velocity profile $f'(\eta)$.

- Figure 4.2 when magnetic parameter M is deccreases with $R > 1$, this behaviour is due to the Lorentz force produced by magnetic field.

- In Figure 4.3 variation in the results of the angle of the wedge β against the velocity $f'(\eta)$ is displayed, with all values of β velocity profile goes upward.

- Figure 4.4 illustrate as the velocity ratio parameter R increases $f'(\eta)$ also rises.

- Figure 4.5 and 4.6 depicts the impact of Pr Prandtl number and Nr radiation parameter. By increasing values of prandtl and reducing values of Nr number in both cases velocity profile decreases.

- Figure 4.7 influences that when convection parameter Bi means the proportion of internal conductive resistance within the body to the outward convective resistance measured at the surface of the body. It is noted that an increase in internal conductive resistance instead of external convective resistance results the improvement in temperature which in return extends the velocity profile $f'(\eta)$.

- Figure 4.8 represent the significant results of Eckert number as Ec increases velocity profile goes downward as $R < 1$ but when $R = 2$ the behaviour is opposite.

- Figure 4.9 illustrate the impact of $(Da)^{-1}$ as Darcy inverse increases at $R = \mathbb{R} - \{1\}$ velocity profile $f'(\eta)$ decreases.

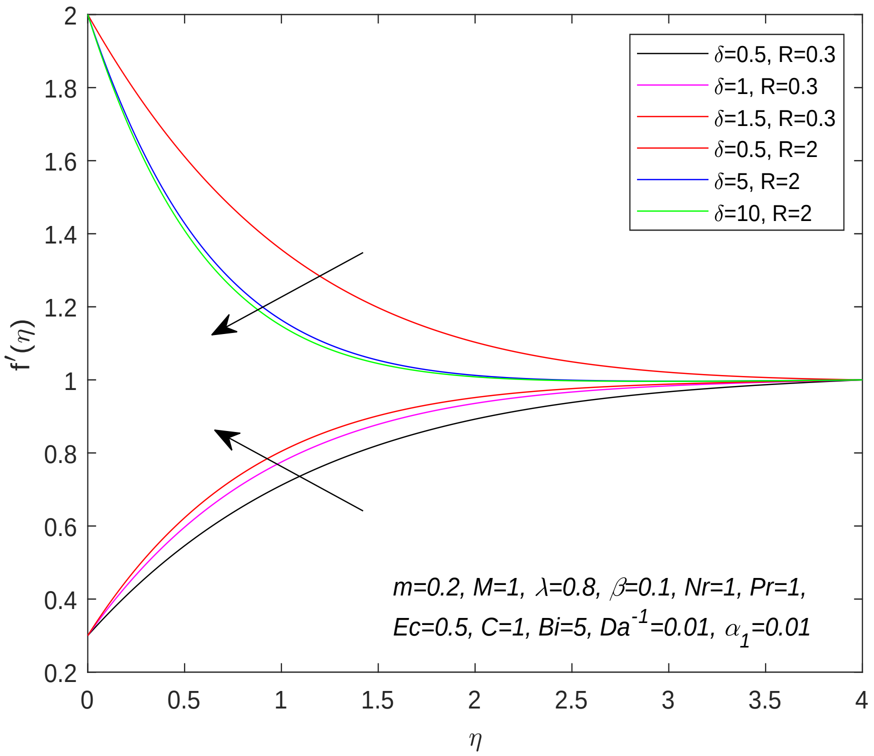

FIGURE 4.1: δ varies on $f'(\eta)$

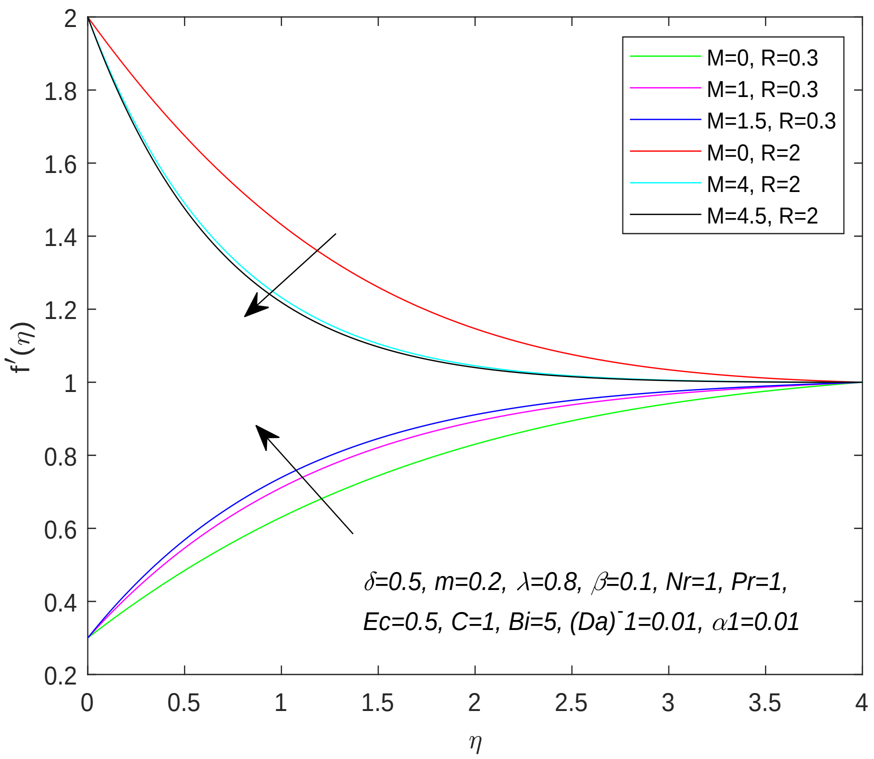

FIGURE 4.2: M varies on $f'(\eta)$

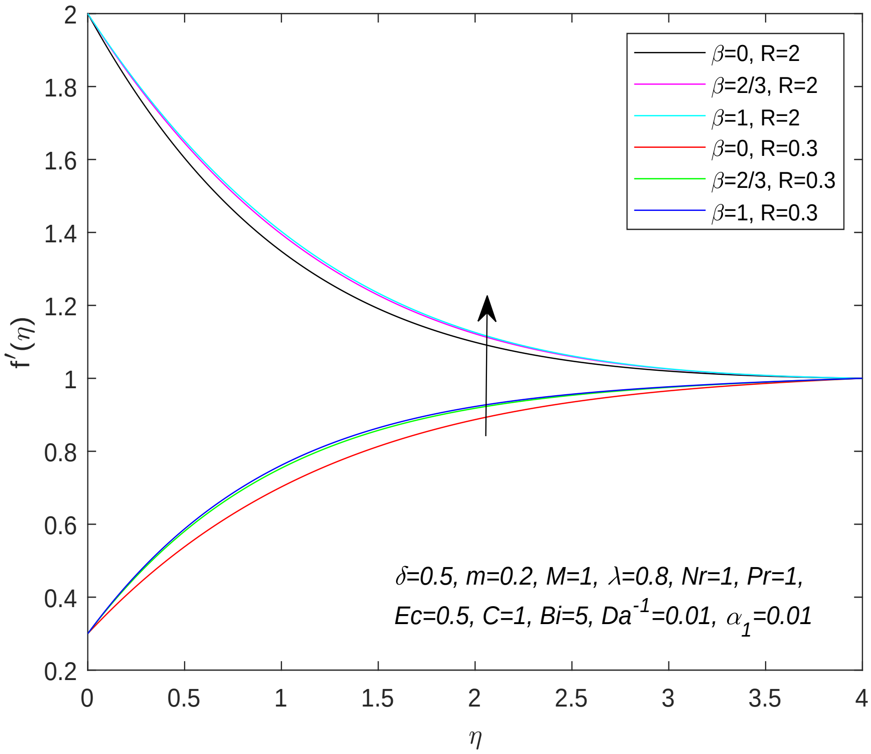

FIGURE 4.3: β varies on $f'(\eta)$

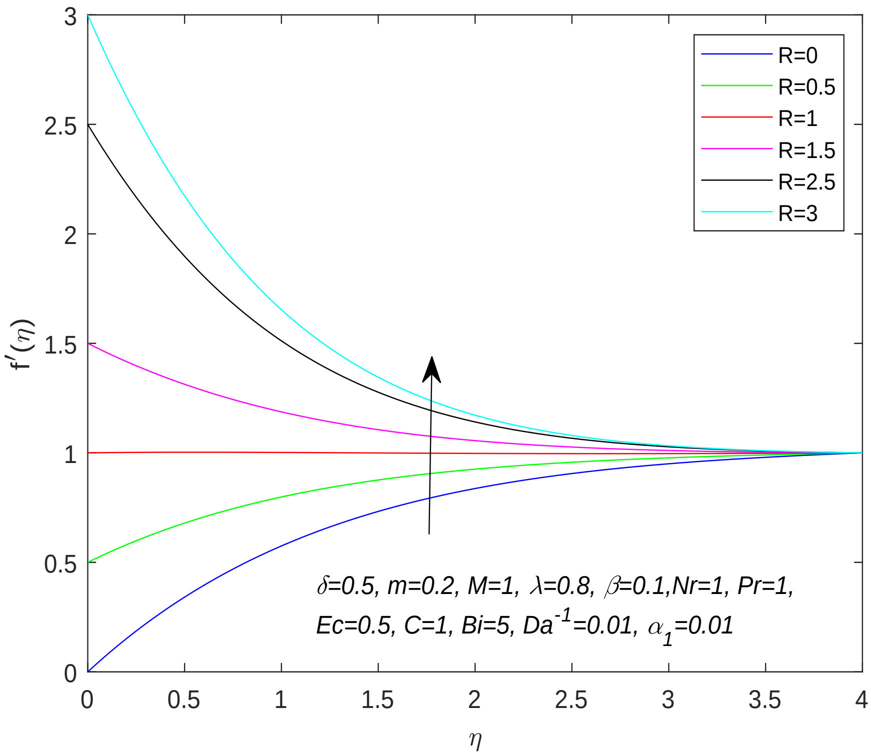

FIGURE 4.4: $f'(\eta)$ for varied values of R

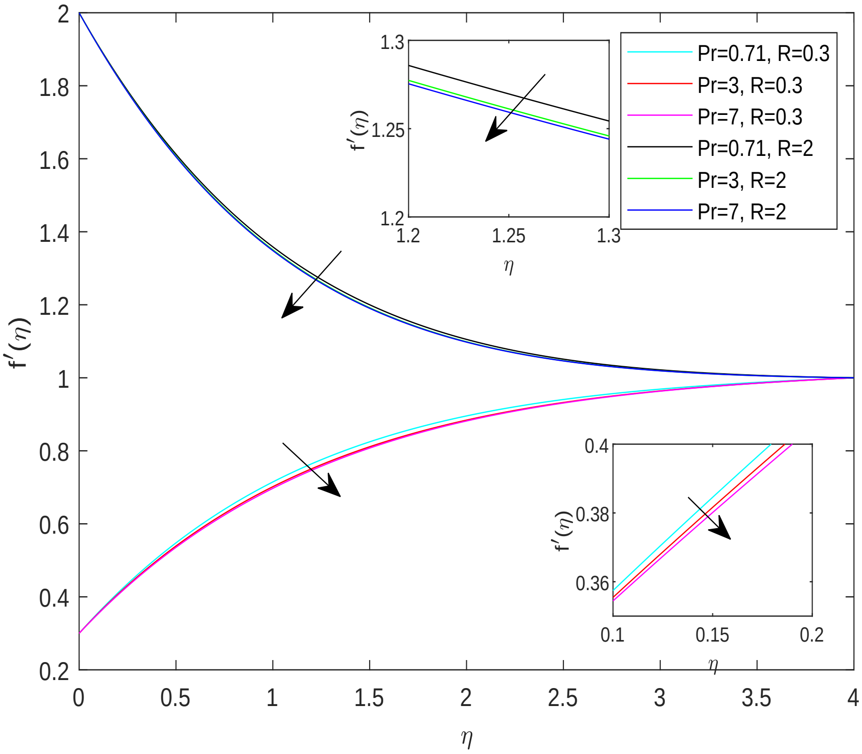

FIGURE 4.5: $f'(\eta)$ for multiple values of Pr

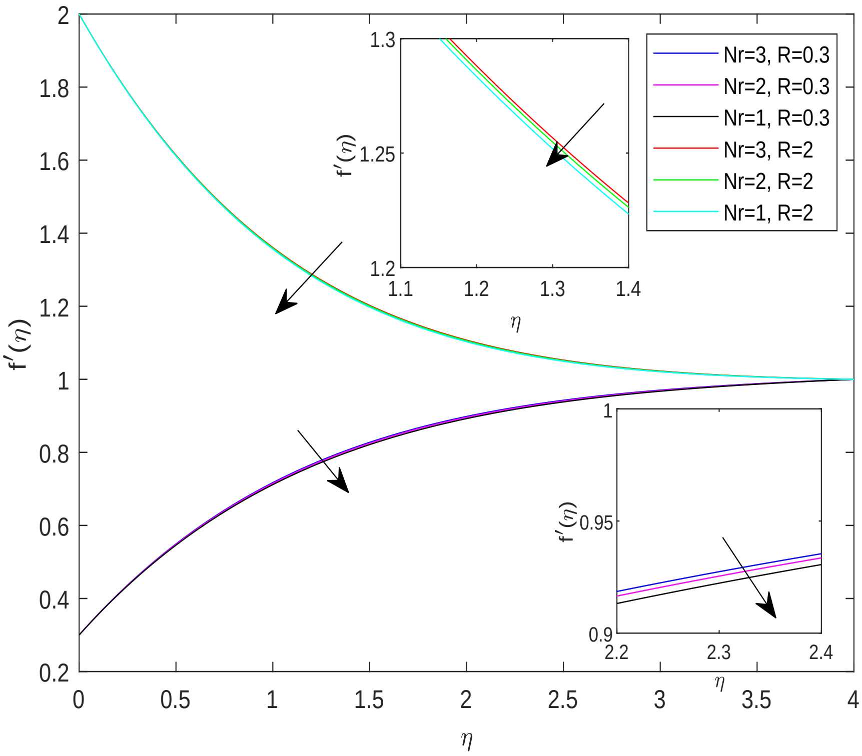

FIGURE 4.6: $f'(\eta)$ for multiple values of Nr

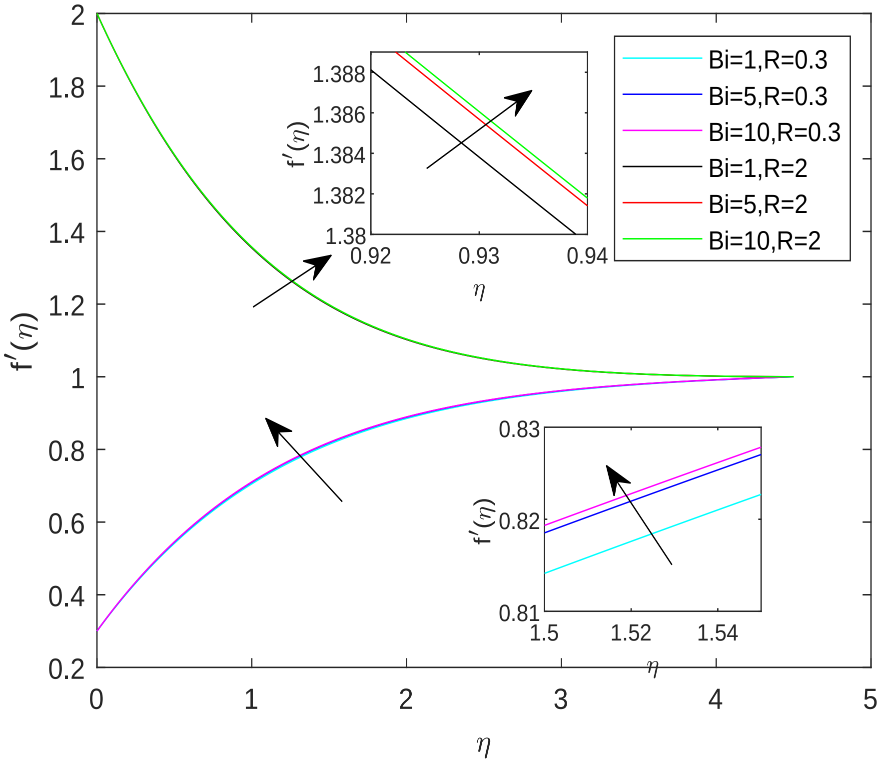

FIGURE 4.7: $f'(\eta)$ for multiple values of B_i

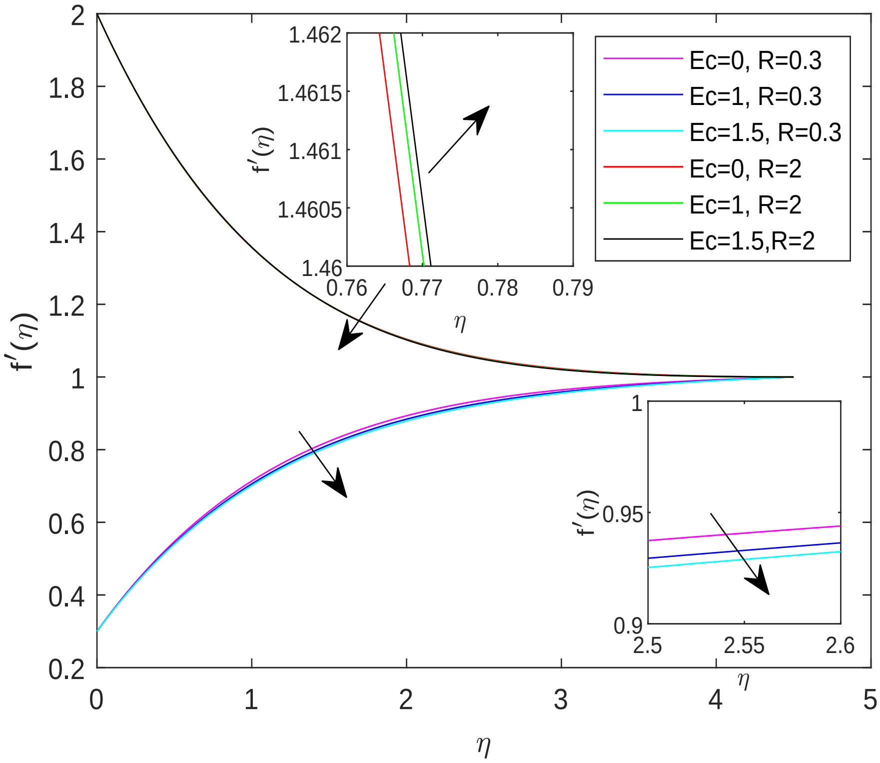

FIGURE 4.8: $f'(\eta)$ for multiple values of Ec

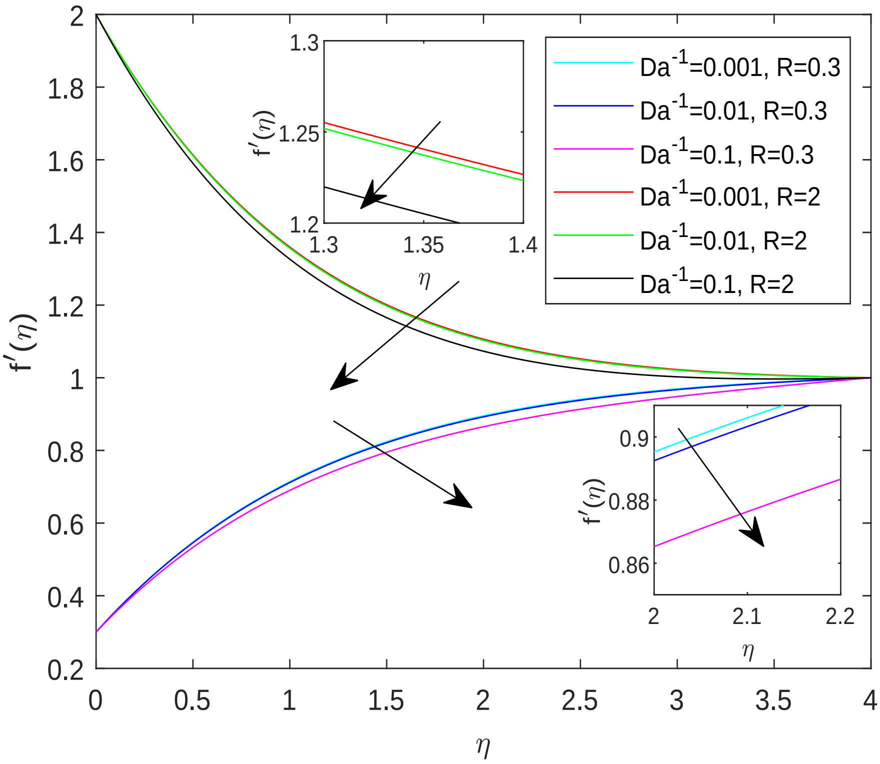

FIGURE 4.9: Velocity profile for different values of $(Da)^{-1}$

4.4.2 The Temperature Profile

- Figure 4.10 exhibits the influence of Casson parameter δ on $\theta(\eta)$ when $R = 0.1$ and $R = 1.5$. In both cases, when $R = \mathbb{R} - \{1\}$, the increase in δ reduce the thickness of temperature profile $\theta(\eta)$.
- Figure 4.11 depicts the results of momentum boundary layer M as for increasing values of M at $R = 0.3$, $\theta(\eta)$ reduces and for $R = 2$, it shows contrary behaviour.
- Figure 4.12 illustrates that at $R = \mathbb{R} - \{1\}$ as wedge angle β rises $\theta(\eta)$ also increases.
- Figure 4.13 shows the behaviour of Nr as by decreasing values of radiation parameter temperature profile $\theta(\eta)$ lessens.
- Figure 4.14 shows the effect of Pr when Prandtl number increases temperature profile $\theta(\eta)$ goes downward.

- Figure 4.15 exhibits the affect of velocity ratio parameter as R goes upward temperature profile $\theta(\eta)$ reduces.
- Figure 4.16 displays the impact of Eckert number as for the increasing values of Ec, $\theta(\eta)$ reduces.
- Figure 4.17 shows the impact of convective number by increasing values of Bi means the proportion of internal conductive resistance within the body to the outward convective resistance measured at the surface of the body. It steeps the behaviour of temperature $\theta(\eta)$, by rising values of conductive heat transfer resistance.
- Figure 4.18 demonstrates when Darcy inverse $(Da)^{-1}$ increases $\theta(\eta)$ also rises.

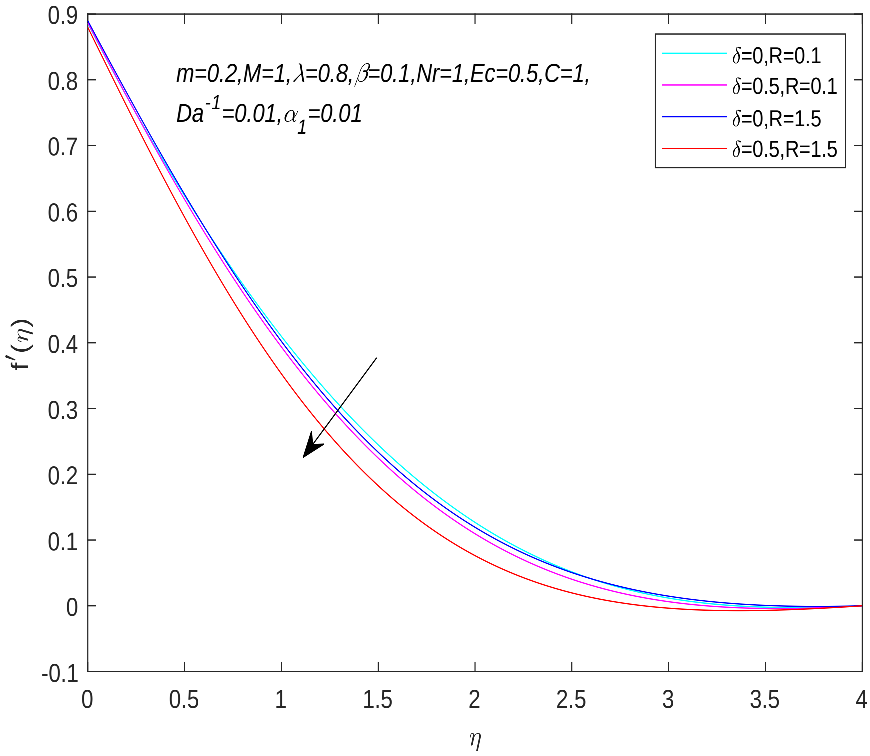

FIGURE 4.10: δ varies in $\theta(\eta)$

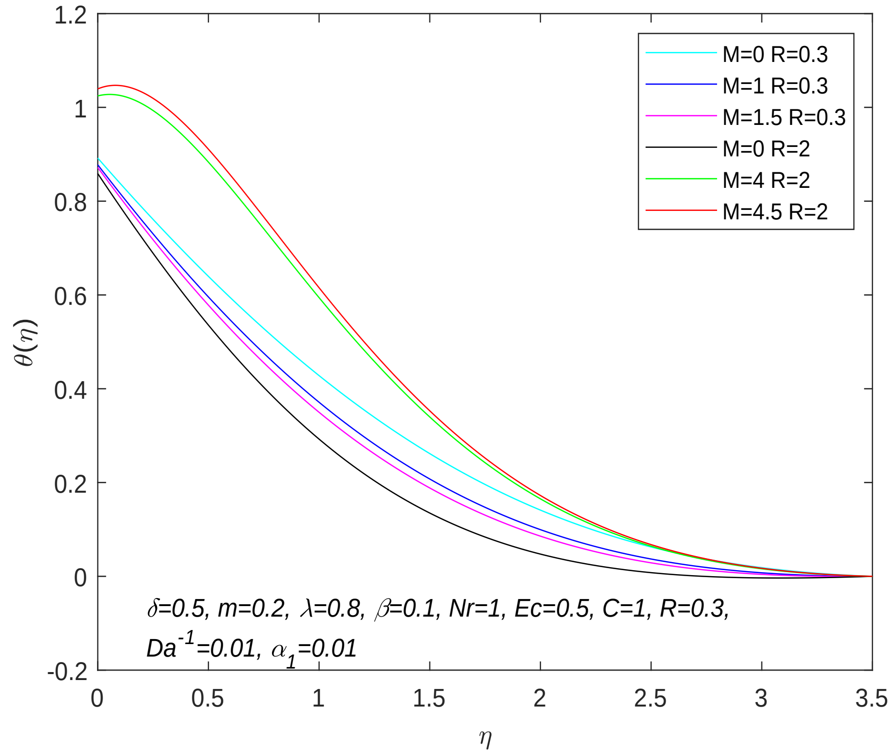

FIGURE 4.11: M varies in $\theta(\eta)$

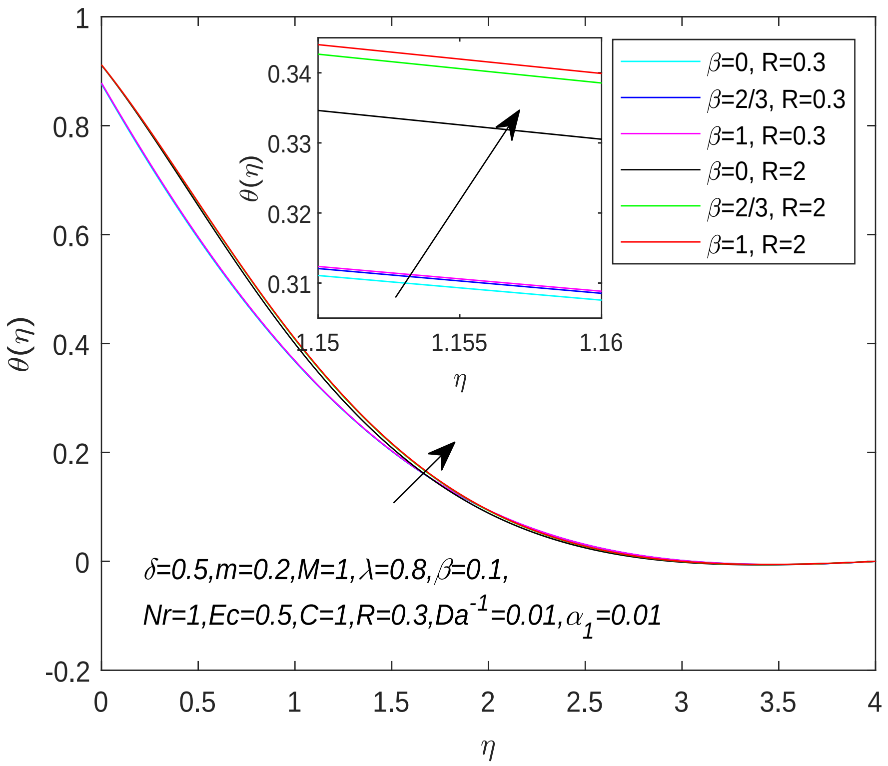

FIGURE 4.12: β varies in $\theta(\eta)$

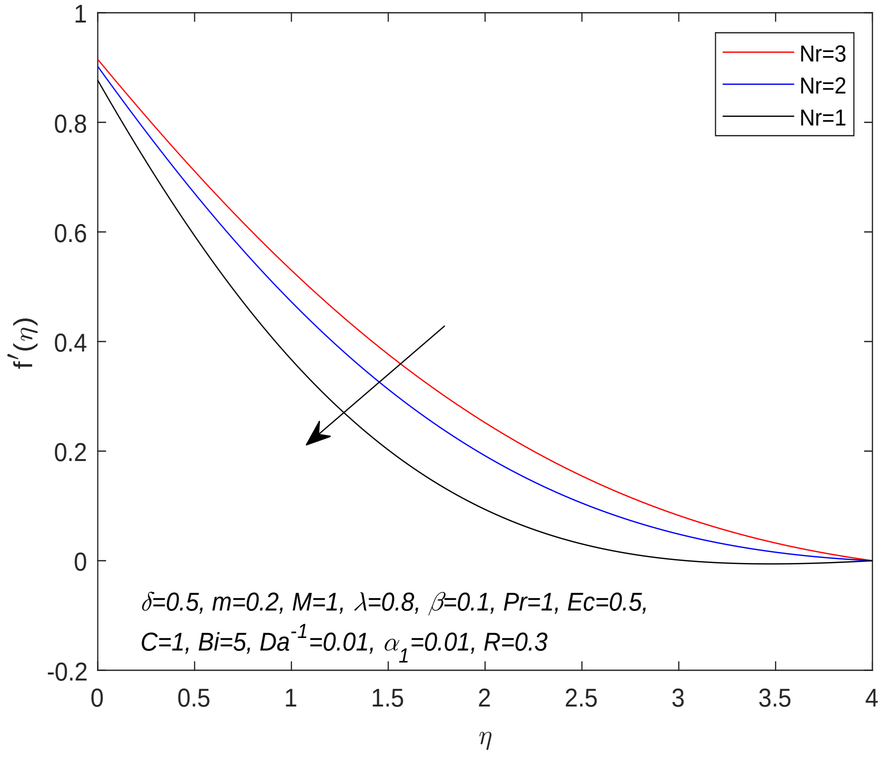

FIGURE 4.13: $\theta(\eta)$ for varied values of Nr

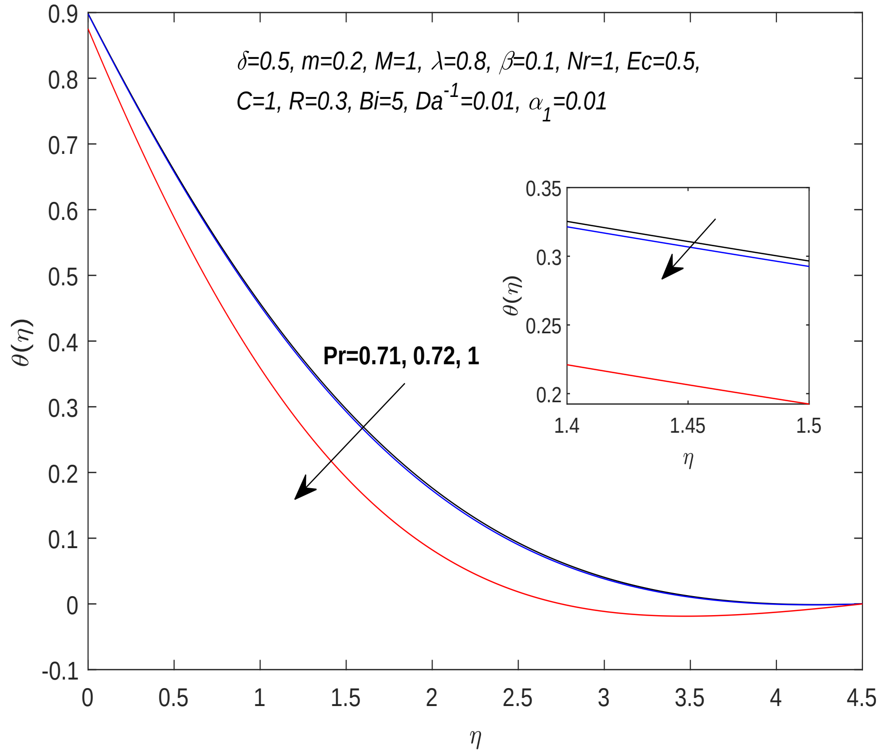

FIGURE 4.14: $\theta(\eta)$ for multiple values of Pr

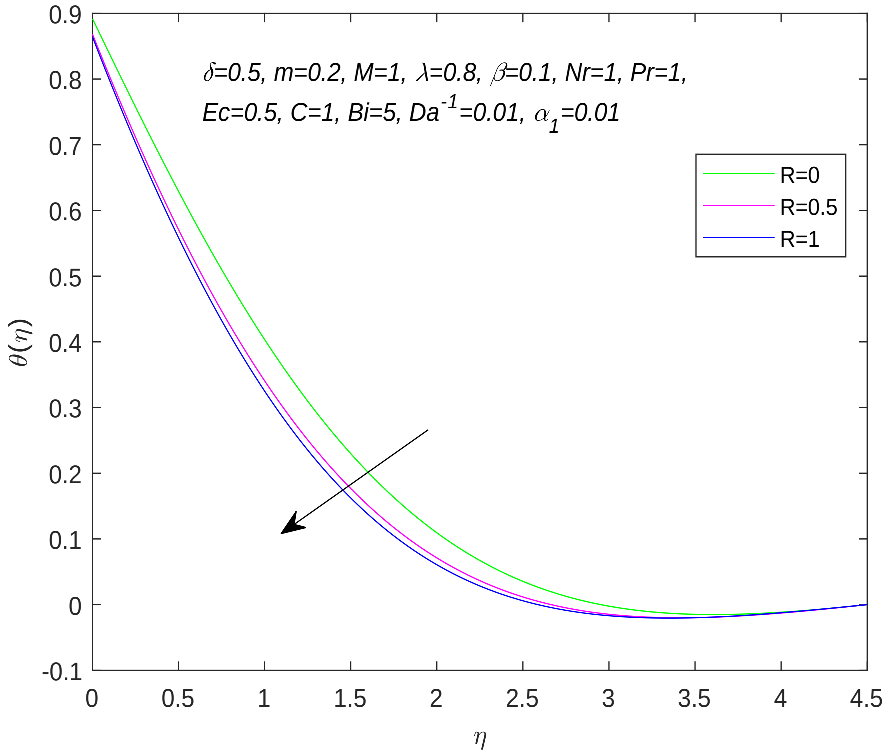

FIGURE 4.15: Temperature profile for varied values of R

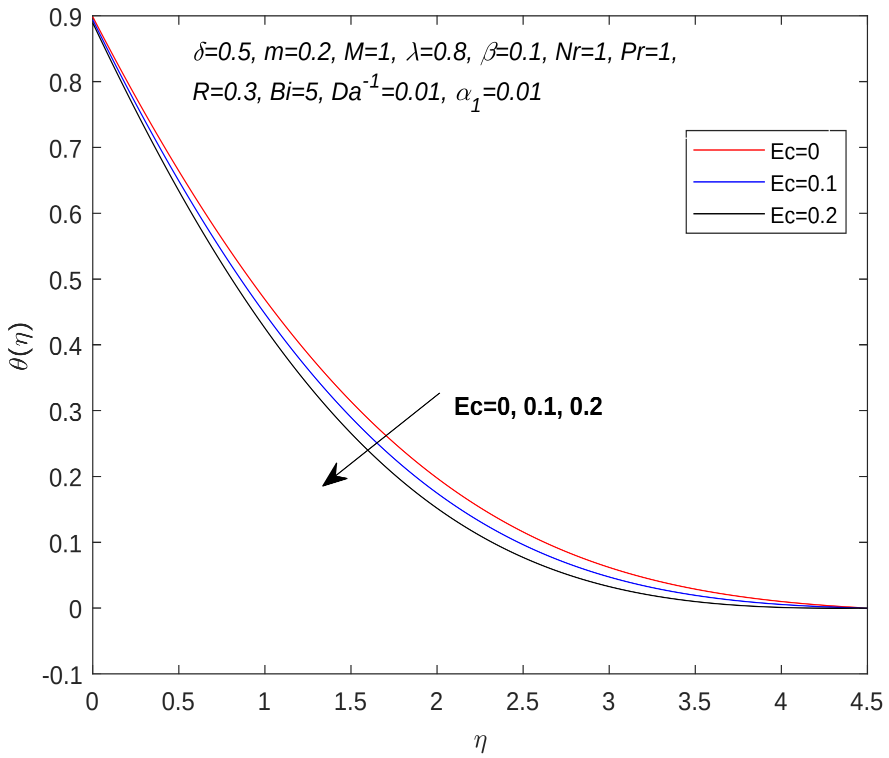

FIGURE 4.16: Temperature profile for different values of Ec

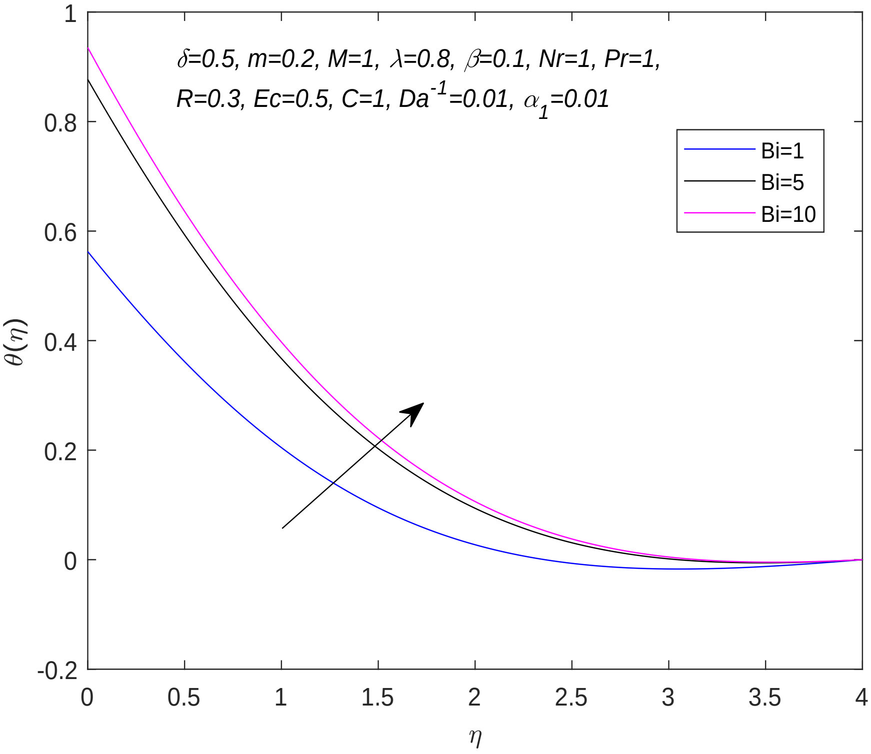

FIGURE 4.17: $\theta(\eta)$ for varied values of B_i

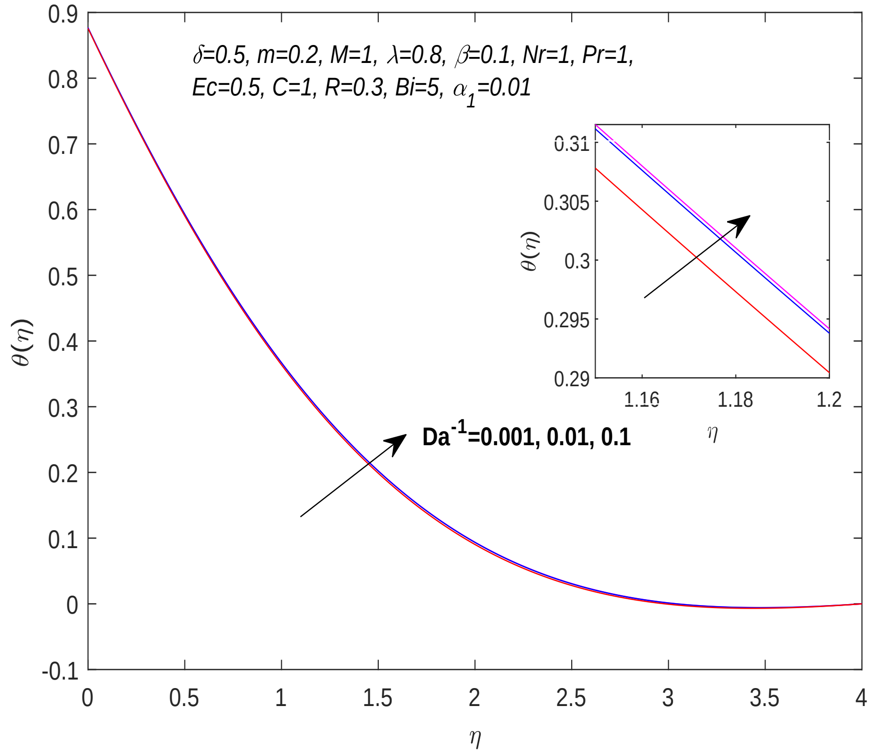

FIGURE 4.18: Temperature profile for various values of $(Da)^{-1}$

4.4.3 Nusselt Number and Surface Drag Force Coefficient

- Figure 4.19 and 4.21 illustrates the impact of convective parameter Bi on Nusselt number $(Re_x)^{\frac{1}{2}}Nu_x$ and skin friction $(Re_x)^{\frac{1}{2}}C_f$ the increasing values of convective parameter, skin friction increases and Nusselt number rises.

- Figure 4.20 and 4.22 depicts the influence of casson parameter on Nusselt number $(Re_x)^{\frac{1}{2}}Nu_x$ and skin friction $(Re_x)^{\frac{1}{2}}C_f$. As the increasing values of δ results an increase in skin friction and a decreases in Nusselt number.

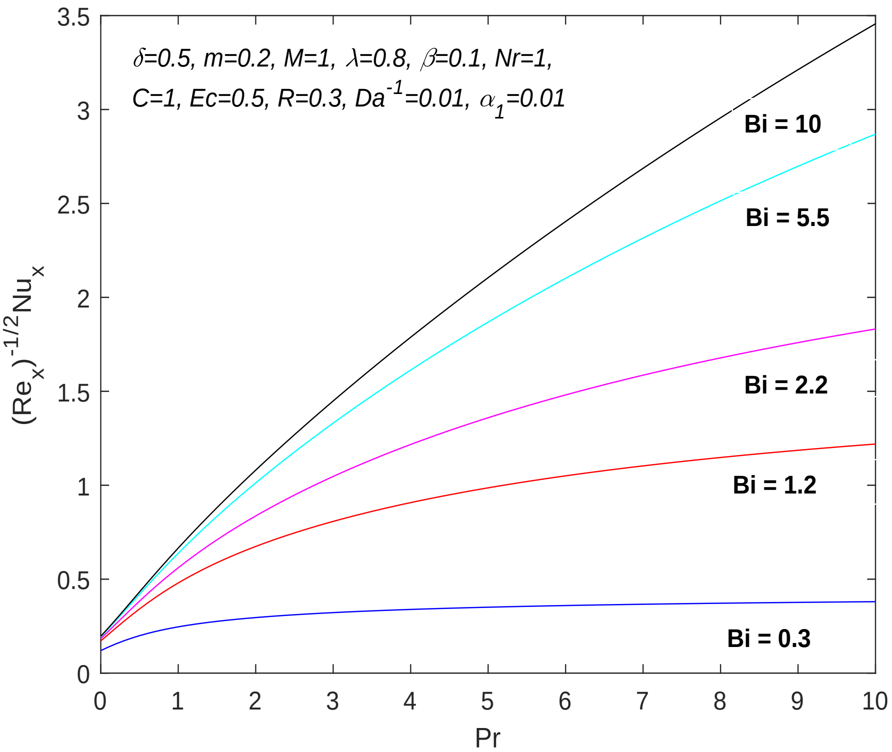

FIGURE 4.19: Nusselt number for various values of B_i

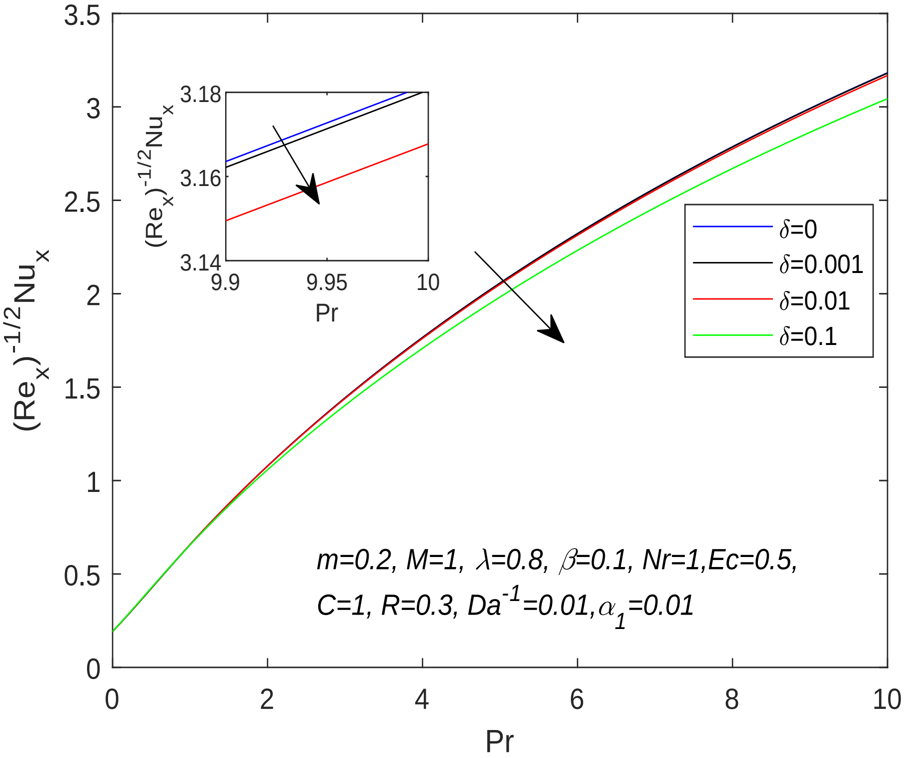

FIGURE 4.20: Nusselt number for different values of δ

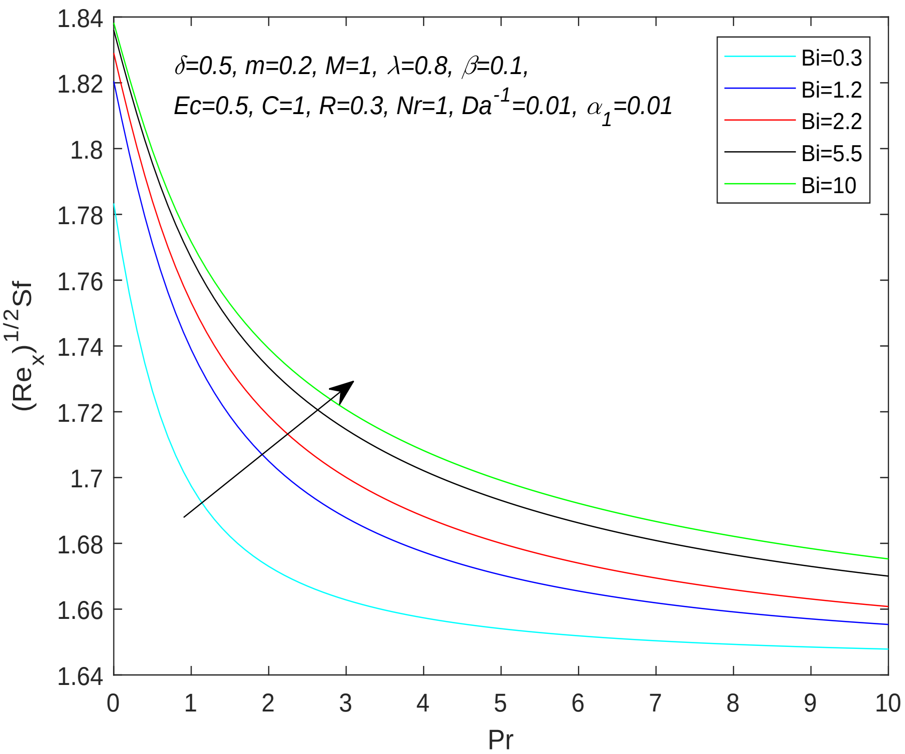

FIGURE 4.21: Surface drag force for varied values of B_i

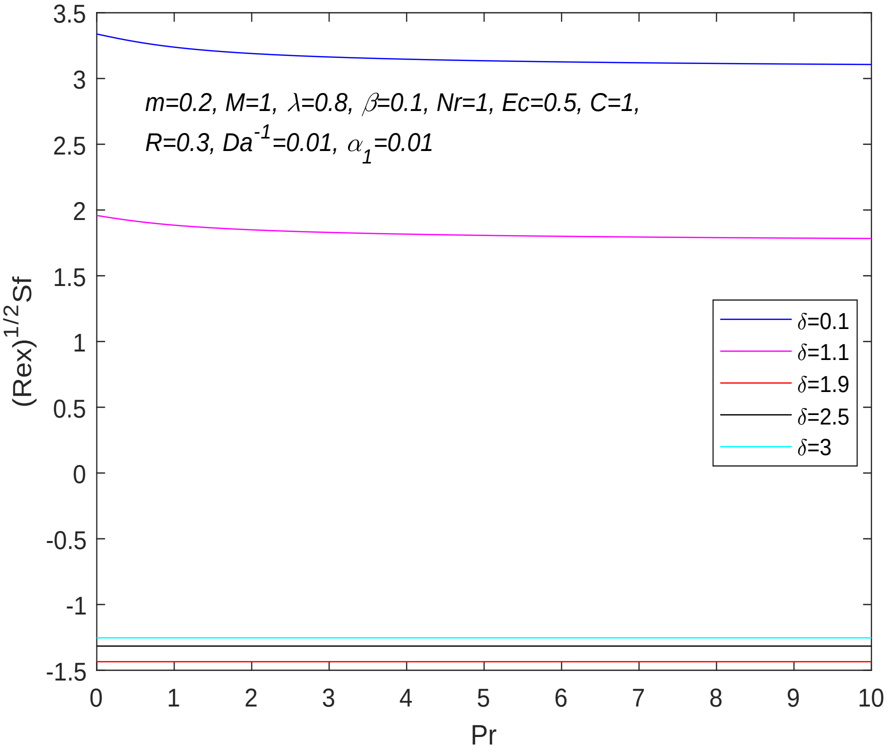

FIGURE 4.22: Surface drag force for varied values of δ

Chapter 5

Conclusion

In present thesis, work of [27] is reviewed and extended by considering diferent terms due to porosity and viscous dissipation. Firstly, using the provided similarity transformations, non-linear PDEs are transformed into non-linear ODEs. After this, these converted equations are numerically solved by using shooting method. Tables and graphs are presented by converting values of various parameters. Following results are notable in graphs:

- As Casson parameter δ increases when $R = 0.3$, $f'(\eta)$ increases and increase in δ when $R = 2$, reduces the thickness of momentum boundary layer.
- When M rises with $R < 1$, $f'(\eta)$ increases and when $R = 2$, $f'(\eta)$ decreases.
- At $R = 0.3$ and $R = 2$, when the Da^{-1} increases the momentum boundary layer decreases.
- As the velocity ratio parameter R increases, $f'(\eta)$ also increases.
- $\theta(\eta)$ increases as δ rises at $R = 0.5$ and $\theta(\eta)$ decreases when $R = 2.1$.
- At $R = 0.3$ and $R = 2$, when the β rises the thermal boundary layer increases.
- It is also observed that with increasing values of Ec the behaviour of temperature profile reduces.

- With an rise in Pr the thermal BL decreases.
- When the value of R rises $\theta(\eta)$ decreases.
- when $(Da)^{-1}$ increases $\theta(\eta)$ also increases.

Bibliography

[1] M. V. Karwe and Y. Jaluria, "Fluid flow and mixed convection transport from a moving plate in rolling and extrusion processes," 1988.

[2] M. Karwe and Y. Jaluria, "Numerical simulation of thermal transport associated with a continuously moving flat sheet in rolling or extrusion," *American Society of Mechanical Engineers, Heat Transfer Division,(Publication) HTD*, vol. 96, pp. 37–45, 1988.

[3] A. Ishak, R. Nazar, and I. Pop, "Mhd mixed convection boundary layer flow towards a stretching vertical surface with constant wall temperature," *International Journal of Heat and Mass Transfer*, vol. 53, no. 23-24, pp. 5330–5334, 2010.

[4] S. Bilal, M. Sohail, R. Naz, M. Malik, and M. Alghamdi, "Upshot of ohmically dissipated darcy-forchheimer slip flow of magnetohydrodynamic sutterby fluid over radiating linearly stretched surface in view of cash and carp method," *Applied Mathematics and Mechanics*, vol. 40, pp. 861–876, 2019.

[5] R. Ravindran, S. Roy, and E. Momoniat, "Effects of injection (suction) on a steady mixed convection boundary layer flow over a vertical cone," *International Journal of Numerical Methods for Heat & Fluid Flow*, vol. 19, no. 3/4, pp. 432–444, 2009.

[6] M. Kumari and G. Nath, "Unsteady mhd mixed convection flow over an impulsively stretched permeable vertical surface in a quiescent fluid," *International Journal of Non-Linear Mechanics*, vol. 45, no. 3, pp. 310–319, 2010.

[7] M. Ganapathirao and R. Ravindran, "Non-uniform slot suction/injection into mixed convective mhd flow over a vertical wedge with chemical reaction," *Procedia Engineering*, vol. 127, pp. 1102–1109, 2015.

[8] I. Ullah, I. Khan, and S. Shafie, "Hydromagnetic falkner-skan flow of casson fluid past a moving wedge with heat transfer," *Alexandria Engineering Journal*, vol. 55, no. 3, pp. 2139–2148, 2016.

[9] M. A. Hossain, N. C. Roy, and S. Siddiqa, "Unsteady mixed convection dusty fluid flow past a vertical wedge due to small fluctuation in free stream and surface temperature," *Applied Mathematics and Computation*, vol. 293, pp. 480–492, 2017.

[10] A. J. Chamkha, M. Mujtaba, A. Quadri, and C. Issa, "Thermal radiation effects on mhd forced convection flow adjacent to a non-isothermal wedge in the presence of a heat source or sink," *Heat and Mass Transfer*, vol. 39, pp. 305–312, 2003.

[11] M. A. Hossain, S. Bhowmick, and R. S. R. Gorla, "Unsteady mixed-convection boundary layer flow along a symmetric wedge with variable surface temperature," *International Journal of Engineering Science*, vol. 44, no. 10, pp. 607–620, 2006.

[12] X. Su, L. Zheng, X. Zhang, and J. Zhang, "Mhd mixed convective heat transfer over a permeable stretching wedge with thermal radiation and ohmic heating," *Chemical Engineering Science*, vol. 78, pp. 1–8, 2012.

[13] R. Kandasamy, I. Muhaimin, and A. B. Khamis, "Thermophoresis and variable viscosity effects on mhd mixed convective heat and mass transfer past a porous wedge in the presence of chemical reaction," *Heat and Mass transfer*, vol. 45, pp. 703–712, 2009.

[14] T. Hayat, M. Hussain, S. Nadeem, and S. Mesloub, "Falkner–skan wedge flow of a power-law fluid with mixed convection and porous medium," *Computers & Fluids*, vol. 49, no. 1, pp. 22–28, 2011.

[15] K. Prasad, P. Datti, and K. Vajravelu, "Mhd mixed convection flow over a permeable non-isothermal wedge," *Journal of King Saud University-Science*, vol. 25, no. 4, pp. 313–324, 2013.

[16] S. A. Gaffar, V. R. Prasad, and E. K. Reddy, "Mixed convection boundary layer flows of a non-newtonian jeffrey's fluid from a non-isothermal wedge," *Ain Shams Engineering Journal*, vol. 8, no. 2, pp. 145–162, 2017.

[17] M. Khan, M. Irfan, L. Ahmad, and W. Khan, "Simultaneous investigation of mhd and convective phenomena on time-dependent flow of carreau nanofluid with variable properties: dual solutions," *Physics Letters A*, vol. 382, no. 34, pp. 2334–2342, 2018.

[18] N. V. Ganesh, A. J. Chamkha, Q. M. Al-Mdallal, and P. Kameswaran, "Magneto-marangoni nano-boundary layer flow of water and ethylene glycol based γ al2o3 nanofluids with non-linear thermal radiation effects," *Case Studies in Thermal Engineering*, vol. 12, pp. 340–348, 2018.

[19] N. V. Ganesh, P. Kameswaran, Q. M. Al-Mdallal, A. Hakeem, and B. Ganga, "Non-linear thermal radiative marangoni boundary layer flow of γal_2o_3 nanofluids past a stretching sheet," Journal of Nanofluids, vol. 7, no. 5, pp. 944–950, 2018.

[20] I. Ullah, S. Shafie, I. Khan, and K. L. Hsiao, "Brownian diffusion and thermophoresis mechanisms in casson fluid over a moving wedge," *Results in Physics*, vol. 9, pp. 183–194, 2018.

[21] S. Bilal, M. Sohail, and R. Naz, "Heat transport in the convective casson fluid flow with homogeneous–heterogeneous reactions in darcy–forchheimer medium," *Multidiscipline Modeling in Materials and Structures*, vol. 15, no. 6, pp. 1170–1189, 2019.

[22] N. V. Ganesh, Q. M. Al-Mdallal, S. Al Fahel, and S. Dadoa, "Riga–plate flow of γ al2o3-water/ethylene glycol with effective prandtl number impacts," *Heliyon*, vol. 5, no. 5, p. e01651, 2019.

[23] N. V. Ganesh, Q. M. Al-Mdallal, and A. J. Chamkha, "A numerical investigation of newtonian fluid flow with buoyancy, thermal slip of order two and entropy generation," *Case Studies in Thermal Engineering*, vol. 13, p. 100376, 2019.

[24] S. Sivasankaran, M. Bhuvaneswari, and A. Alzahrani, "Numerical simulation on convection of non-newtonian fluid in a porous enclosure with non-uniform heating and thermal radiation," *Alexandria Engineering Journal*, vol. 59, no. 5, pp. 3315–3323, 2020.

[25] M. Sohail, R. Naz, and S. I. Abdelsalam, "Application of non-fourier double diffusions theories to the boundary-layer flow of a yield stress exhibiting fluid model," *Physica A: Statistical Mechanics and its Applications*, vol. 537, p. 122753, 2020.

[26] M. Sohail, Z. Shah, A. Tassaddiq, P. Kumam, and P. Roy, "Entropy generation in mhd casson fluid flow with variable heat conductance and thermal conductivity over non-linear bi-directional stretching surface," *Scientific Reports*, vol. 10, no. 1, p. 12530, 2020.

[27] M. Hussain, A. Ghaffar, A. Ali, A. Shahzad, K. S. Nisar, M. Alharthi, and W. Jamshed, "Mhd thermal boundary layer flow of a casson fluid over a penetrable stretching wedge in the existence of nonlinear radiation and convective boundary condition," *Alexandria Engineering Journal*, vol. 60, no. 6, pp. 5473–5483, 2021.

[28] A. Aziz, "A similarity solution for laminar thermal boundary layer over a flat plate with a convective surface boundary condition," *Communications in Nonlinear Science and Numerical Simulation*, vol. 14, no. 4, pp. 1064–1068, 2009.

[29] J. M. Cimbala and Y. A. Cengel, *Fluid mechanics: fundamentals and applications.* McGraw-Hill Higher Education, 2006.

[30] R. Bansal, *A textbook of fluid mechanics.* Firewall Media, 2005.

[31] B. Lautrup, *Physics of continuous matter: exotic and everyday phenomena in the macroscopic world*. CRC press, 2011.

[32] C. Kothandaraman, *Fundamentals of heat and mass transfer*. New Age International, 2006.

[33] R. Dash, K. Mehta, and G. Jayaraman, "Casson fluid flow in a pipe filled with a homogeneous porous medium," *International Journal of Engineering Science*, vol. 34, no. 10, pp. 1145–1156, 1996.

[34] S. S. Molokov, R. Moreau, and H. K. Moffatt, *Magnetohydrodynamics: Historical evolution and trends*, vol. 80. Springer Science & Business Media, 2007.

[35] J. N. Reddy and D. K. Gartling, *The finite element method in heat transfer and fluid dynamics*. CRC press, 2010.

[36] J. Kunes, *Dimensionless physical quantities in science and engineering*. Elsevier, 2012.

[37] F. Mabood, S. Ibrahim, M. Rashidi, M. Shadloo, and G. Lorenzini, "Non-uniform heat source/sink and soret effects on mhd non-darcian convective flow past a stretching sheet in a micropolar fluid with radiation," *International Journal of Heat and Mass Transfer*, vol. 93, pp. 674–682, 2016.